Neuraminidase B controls neuraminidase A-dependent mucus production and evasion

Short title: Role of neuraminidases in pneumococcal-mucus interactions

Alexandria J. Hammond[1], Ulrike Binsker[1*], Surya D. Aggarwal[1], Mila Brum Ortigoza[1,3], Cynthia Loomis[2], Jeffrey N. Weiser[1]

[1]Department of Microbiology, New York University School of Medicine, New York, NY, United States of America

[2]Department of Pathology, New York University School of Medicine, New York, NY, United

[3]Department of Medicine, Division of Infectious Diseases, New York University School of Medicine, New York, NY, United States of America States of America

* Department for Biological Safety, Federal Institute for Risk Assessment, Berlin, Germany

Corresponding author

E-Mail: Jeffrey.Weiser@nyulangone.org (JNW)

Conflict of interest statement

The authors have declared that no conflict of interest exists.

Abstract

Binding of *Streptococcus pneumoniae* (Spn) to nasal mucus leads to entrapment and clearance via mucociliary activity during colonization. To identify Spn factors allowing for evasion of mucus binding, we used a solid-phase adherence assay with immobilized mucus of human and murine origin. Spn bound large mucus particles through interactions with carbohydrate moieties. Mutants lacking neuraminidase (*nanA*) or neuraminidase B (*nanB*) showed increased mucus binding that correlated with diminished removal of terminal sialic acid residues on bound mucus. The non-additive activity of the two enzymes raised the question why Spn expresses two neuraminidases and suggested they function in the same pathway. Transcriptional analysis demonstrated expression of *nanA* depends on the enzymatic function of NanB. As transcription of *nanA* is increased in the presence of sialic acid, our findings suggest that sialic acid liberated from host glycoconjugates by the secreted enzyme NanB induces the expression of the cell-associated enzyme NanA. The absence of detectable mucus desialylation in the *nanA* mutant, in which NanB is still expressed, suggests that NanA is responsible for the bulk of the modification of host glycoconjugates. Thus, our studies describe a functional role for NanB in sialic acid sensing in the host. The contribution of the neuraminidases *in vivo* was then assessed in a murine model of colonization. Although mucus-binding mutants showed an early advantage, this was only observed in a competitive infection, suggesting a complex role of neuraminidases. Histologic examination of the upper respiratory tract demonstrated that Spn stimulates mucus production in a neuraminidase-dependent manner. Thus, an increase production

of mucus containing secretions appears to be balanced, *in vivo*, by decreased mucus binding. We postulate that through the combined activity of its neuraminidases, Spn evades mucus binding and mucociliary clearance, which is needed to counter neuraminidase-mediated stimulation of mucus secretions.

Author Summary

Streptococcus pneumoniae (Spn) is a leading mucosal pathogen, whose host interaction begins with colonization of the upper respiratory tract. While there has been extensive investigation into bacterial interaction with epithelial cells, there is little understanding of bacterial-mucus interactions. Our study used mucus of human and murine origin and a murine model of colonization to study mucus associations involving Spn. The main findings reveal i) the enzymatic activity of Spn's neuraminidases (NanA and NanB) contribute to mucus evasion through removing terminal sialic acid, ii) the enzymatic activity of NanB controls expression of the main neuraminidase, NanA, and iii) Spn induces sialic acid containing mucus secretions *in vivo* in a neuraminidase-dependent manner. We postulate that during colonization, neuraminidase-dependent reduction in mucus binding enables evasion of mucociliary clearance, which is necessary to counter neuraminidase-mediated stimulation of mucus secretions. Thus, our study provides new insights into the role of Spn neuraminidases on colonization.

Introduction:

The human nasopharynx contains a diverse and extensive microbial flora, which includes *Streptococcus pneumoniae* (Spn or the pneumococcus). Spn colonization of the upper respiratory tract (URT) is typically asymptomatic. However, transit of Spn to normally sterile sites can cause a broad spectrum of disease including otitis media, pneumonia, sepsis and meningitis (1). Regardless of the disease manifestation, successful colonization of URT is the critical first step in Spn pathogenesis.

Colonizing pneumococci are found in intimate contact with the glycocalx, the layer of mucus that coats the surfaces of the URT (2). The major macro-molecular constituents of mucus are mucins, a heterogeneous family of heavily glycosylated proteins that form biopolymer gels through hydrophobic interactions (3). This layer provides a barrier protecting the underlying epithelial surface from pathogens and mechanical damage. An additional characteristic of mucins are their anionic properties due in large part to extensive sialylation of their terminal glycans (4). The association between Spn and mucus could promote its retention along the mucosal surface or, alternatively, allow for clearance through the mucociliary flow that continuously sweeps the URT. Mucus also enhances replication within the nutrient poor environment of the mucosal surface, by providing Spn a source of carbohydrates, including sialic acid, cleaved from mucin glycans (14,40).

Although Spn resides in the mucus layer and is considered an opportunistic mucosal pathogen, there has been minimal investigation into bacterial-mucus interactions. The physical characteristics of mucus: insolubility, heterogeneity and adhesive properties, make it particularly difficult to study both *in vitro* and *in vivo*. Earlier work has shown that Spn is found associated with luminal mucus during the first few

hours following acquisition, before transiting to the glycocalyx, where stable colonization of the epithelial surface occurs (2).

Spn's main virulence factor is a thick polysaccharide capsule, which inhibits adherence to immobilized mucus glycoproteins and during colonization, allowing for escape from luminal mucus (16,2). This corresponds with attenuated colonization of unencapsulated pneumococcal strains, demonstrating the importance of mucus interactions for colonization (2). This effect of capsule in blocking mucus interactions could be due to repulsion by capsular polysaccharides, which are anionic for all but a few serotypes, with negatively-charged mucus. To examine whether other pneumococcal surface factors affect bacterial-mucus interactions, our lab developed a solid phase adherence assay to look directly at the interactions between Spn and nasal secretions obtained from humans (hNF, human nasal fluid) (5). Results from this assay demonstrated that Spn adherence to hNF was dominant among pneumococcal isolates expressing type-1 pilus. Pilus-1-dependent binding required naturally-acquired secretory immunoglobulin A (S-IgA) that binds to the type-1 pilus which led to bacterial agglutination in mucus. Recognition by specific antibody correlated with enhanced pilus-1-dependent Spn clearance in a mouse model of URT colonization when Spn were pre-treated with human S-IgA (immune exclusion). These results could explain the lower prevalence of the pilus-1 locus in isolates from adults who have accumulated naturally-acquired secretory antibody.

The purpose of this study is to determine if other pneumococcal surface factors or enzymes affect interactions with host mucus, impacting acquisition and persistence of colonization. In particular, we analyzed the effects of surface exoglycosidases, which

have been previously shown to act on host glycoconjugates (6). These cleavage events have been shown to expose epithelial cell receptors for adherence, modulate host factors involved in clearance and allow for nutrient acquisition (6, 12,14,15). However, it remains unclear how these glycosidases affect mucus binding and contribute to mucus-mediated clearance.

The pneumococcal factors found to be important in adherence to mucus include the neuraminidases A and B. Remarkably, we observed that the expression of *nanA* depends on the enzymatic activity of NanB and that Spn neuraminidases promote mucus production during murine colonization. Our study highlights the importance of sialic acid removal for Spn interactions with mucus both *in vitro* and *in vivo*.

Results:

Pneumococcal adherence to upper respiratory airway contents

To avoid the confounding effects of anti-pilus S-IgA, we used murine URT lavages as a source of material to look at pneumococcus-mucus interactions. URT lavages were pooled from adult mice to control for mouse to mouse variation. The association of Spn with immobilized pooled murine nasal lavages (mNLs) was quantified through a solid-phase adherence assay with BSA as a blocking reagent. Prior to immobilization, mNLs were sonicated for homogenization and we noticed with increased sonication time, adherence of the Type 4 TIGR4 isolate was reduced (Fig. 1A). To confirm that Spn bound to large mucus particles, we showed that prefiltering (0.45 micron) of mNLs significantly reduced binding (Fig. 1B). Next, mNLs were treated with trypsin or sodium periodate to determine if Spn was binding to proteinaceous or

carbohydrate structures, respectively (Fig. 1C, D). A significant reduction in adherence was only seen with sodium periodate treatment. Lastly, to confirm that Spn was interacting with mucus particles in mNLs, we performed microscopy with alcian blue dye, which stains mucus polysaccharides (Fig. 1E, F). Pneumococci were associated with small alcian blue staining globules (Fig. 1E). Spn bound to mucoid globules in mNLs were predominantly in long chains as compared to unbound bacteria (Fig. 1E). Increased chain length, which increases surface area per bacterial particle, has been positively associated with pneumococcal adherence and colonization (22). These experiments demonstrated that Spn binds to mucus-containing particles in the URT.

Screening pneumococcal surface factors for their effect on mucus interactions

We focused on pneumococcal surface factors that had been shown, or hypothesized, to interact with mucus (2,5,6,24,25,8). Of the four surface factors (genes) initially tested using deletion mutants: capsule (*cps*), type-1-pilus (*rlrA*), choline binding protein A (*cbpA*) and mucin binding protein (*mucBP*) were tested for their contribution to adherence to mNLs, only capsule (*cps)* affected Spn's interactions with mucus in the solid phase binding assay (Table 1, Fig. 2 A, B). The increased adherence by the unencapsulated mutant was consistent with other published results using different mucus adherence assays (2). The lack of an effect for RlrA was expected, as mNLs lack naturally-acquired anti-pilus S-IgA (Fig. 2B) (5).

Next, we tested pneumococcal surface enzymes for their role in mucus binding (Table 1). We saw no effect of the O-deacetylase EstA, which acts on sialic acid residues; no effect of StrH, an exoglycosidase that cleaves terminal β1-linked N-

163 acetylglucosamine; and a strain-specific effect with BgaA, an exoglycosidase which
164 cleaves terminal beta-galactose and, consequently, these genes were not considered
165 further (45, 46, 8).

166 **Table 1:**
167 **Spn surface factors tested for their effect on mucus interactions**

SP_#	Gene Name	Gene Function	Increase adherence (mNL)
SP_0461-0468	*rlrA*	Type 1 pilus; Adhesin	-
SP_2190	*cbpA/pspC*	Choline binding protein A; Adhesion to pIGR, binds human secretory component	-
SP_0342-0366	*cps*	Capsule; Capsule biosynthesis	+
SP_1492	*mucBP*	Mucin binding protein	-

168
169 **Spn enzymes tested for their effect on mucus interactions**

SP_#	Gene Name	Gene Function	Increase adherence (mNL)
SP_0614	*estA*	O-deacetylase; Removes acetyl groups from sialic acid facilitating neuraminidase activity	-[#]
SP_1693	*nanA*	Neuraminidase; Exo-glycosidase, binds and releases terminal α2,3 and α2,6 sialic acid	+[Ψ]
SP_1687	*nanB*	Neuraminidase; Exo-glycosidase, binds and releases terminal α2,3 sialic acid	+
SP_0648	*bgaA*	B-galactosidase; Binds and releases β1-4 galactose	-[*]
SP_0057	*strH*	N-acetylhexosaminidase; Binds and releases N-acetylglucosaminidase	-[~]

170 [*]Strain-dependent, strain Type 23F (Yes), TIGR4 (No)

171 Ψ Effect observed with Type 23F. No significant effect in strain TIGR4 which expresses a
172 truncated, secreted form of the enzyme
173 ˜Only tested in the Type 23F background
174 # Additionally, tested in hNF due to the difference in acetylation in humans versus mice (28)
175

176 Pneumococcal neuraminidases negatively affect binding to mucus

177 Neuraminidases are exoglycosidases, which cleave terminal sialic acid
178 (neuraminic acid), including on residues found within host glycoconjugates.
179 Neuraminidases are found in all pneumococcal strains, and are encoded by three
180 different genes *nanA, nanB* and *nanC*. NanA, which cleaves α2,3- α2,6- and α2,8-linked
181 sialic acid, is present in all strains, while NanB and NanC, with specificity for α2,3-linked
182 sialic acid, are expressed by 96% and 51% of strains, respectively (9-11). The function
183 of neuraminidases has been attributed to release of sialic acid for nutrition or for
184 promoting adherence to epithelial cell receptors which become exposed upon removal
185 of sialic acid (13,6,12,14). Spn neuraminidases have also been shown to desialylate the
186 surface of other microbes that reside in the human URT potentially providing a
187 competitive advantage (49).

188
189 NanA, of the extensively studied TIGR4 isolate, contains a frameshift mutation 5'
190 to the domain expressing the LPxTG-cell wall anchoring motif, resulting in secretion of
191 the enzymatic portion of the protein (20). As this mutation is an anomaly among
192 pneumococci, we investigated the neuraminidase's role in mucus interactions using an
193 isolate of Type 23F that lacks *nanC* (9). In addition to testing adherence in mNLs, we
194 used hNF pooled from healthy adults as a more physiologic substrate, since Spn
195 resides along the mucosal surface of the human URT. In order to detect robust mucus
196 binding to hNF, we utilized a previously described Type 23F isolate with an inserted

type-1 pilus (Type 23F::pilus-1) and confirmed its robust adherence to hNF in our assay (Fig. 2C) (5). Binding of the Type 23F ∇pilus-1 to large mucus particles in hNF was confirmed using alcian blue staining (Fig. 1F). Construction of an unmarked, in-frame deletion of *nanB* resulted in a ~5-fold increase in adherence to mNL that was fully corrected in the chromosomally complemented strain (Fig 3A). The *nanB*::janus knockout mutant strain also displayed a ~2.5 fold increase in adherence to hNF (Fig. 3B). NanB contains both an enzymatic and lectin binding domain (21). To determine the role of the former in mucus adherence, we constructed a mutant with an enzymatically inactive NanB ($NanB_{D270A}$). To generate this strain, we mutated an aspartic acid residue, a conserved feature of sialidase active sites, which is an acid/base catalyst situated within a loop adjacent to the active site (21). The enzymatically inactive strain ($NanB_{D270A}$) demonstrated significantly increased adherence to hNF compared to wild-type controls, confirming that the enzymatic activity of NanB is responsible for mucus evasion (Fig. 3C). Next, we tested an unmarked, in-frame deletion of *nanA* and chromosomally-corrected mutant to test for adherence to mNL and hNF (Fig. 3D, E). We observed a similar increase in adherence in the *nanA*-deficient strain with both substrates (mNL and hNF) that was fully corrected in the complemented strain (Fig. 3D, E). To determine if there was an additive effect of NanA and NanB in mucus binding, we tested a double Δ*nanA, nanB*::janus mutant for adherence to hNF (Fig. 3B). Interestingly, the double mutant showed comparable adherence levels to the *nanB* single mutant. This suggested that there was no additive effect of the two neuraminidases in mucus binding, and raised the possibility that they function in the same pathway.

220 NanB regulates *nanA* in a sialic acid-dependent manner

221 To better understand the relationship between the two neuraminidases, we first
222 validated the loss of enzymatic activity in our mutants using a sensitive neuraminidase
223 activity assay. The Type 23F isolate showed moderate levels of cell-associated
224 neuraminidase activity compared to other clinical isolates and as predicted this level
225 was reduced for strain TIGR4 that expresses a secreted version of NanA (Fig. 4A). We
226 noted high levels of neuraminidase activity for the parent strain, and the chromosomally-
227 corrected mutants of *nanA* and background levels of activity for the deletion mutant of
228 *nanA (*Fig. 4B). Surprisingly, no appreciable levels were observed for the *nanB* deletion
229 and the $NanB_{D270A}$ mutant, both of which still encode for *nanA*. Correction of the *nanB*
230 mutant restored normal levels of neuraminidase activity. Further, the double
231 neuraminidase mutant also did not display any neuraminidase activity. The inactivation
232 of either *nanA* or *nanB,* therefore, was sufficient to eliminate completely neuraminidase
233 activity, further supporting the hypothesis/finding that the these enzymes might function
234 in the same pathway (Fig. 4B).

235 Next, we compared transcription of the neuraminidase genes during *in vitro*
236 growth in nutrient rich media to determine how *nanA* and *nanB,* which are expressed on
237 separate transcriptional units in the same genetic locus, might interact (23). *NanB*
238 expression was as anticipated, with no difference in expression observed between the
239 parental strain, *nanA*-deletion and $NanB_{D270A}$ mutants (Fig. 4C). *NanB* was not
240 transcribed in the *nanB*-deletion mutant and double neuraminidase mutant strains. As
241 expected, the *nanA* transcript was not detected in the *nanA*-deletion mutant and double
242 neuraminidase mutant, but surprisingly the *nanA* transcript was also not detected in the

243 *nanB*-deletion mutant (FIG. 4D). The $NanB_{D270A}$ mutant in which the catalytically inactive
244 form of *nanB* is transcribed also lacked *nanA* transcripts, suggesting that the enzymatic
245 function of NanB is necessary for *nanA* expression. As transcription of *nanA* is
246 increased in response to the presence of free sialic acid and controlled by the positive
247 regulator NanR, we checked expression levels of *nanR* under these growth conditions
248 (Fig. 4E) (23). Expression of *nanR* was unaffected by the expression of function NanA
249 or NanB, suggesting that the enzymatic activity of NanB regulates *nanA* through post-
250 transcriptional effects on the NanR regulator. We then provided a host source of sialic
251 acid to test NanB regulation of *nanA* under the conditions used in our adherence assay
252 (Fig. 4F). Neuraminidase activity in DMEM was increased by addition of mNL as the
253 source of sialic acid and this effect was not due to increased bacterial growth. Again,
254 neuraminidase activity was dependent on the presence of *nanB* and the enzymatic
255 activity of NanB. Together these observations were consistent with the use of host
256 glycoconjugates from the URT by Spn as a source of sialic acid and that this sialic acid
257 is liberated by NanB to trigger expression of *nanA*.
258
259 <u>Spn neuraminidases exert their effect on mucus through desialylation</u>
260 To verify that increased mucus binding was based on the neuraminidase activity
261 of Spn, we pre-treated immobilized hNF using *Vibrio cholerae* neuraminidase (Fig. 5A).
262 Pre-treatment with exogenous neuraminidase complemented the phenotype of
263 increased adherence compared to vehicle controls of the single and double *nanA* and
264 *nanB* mutants, confirming the role of sialic acid removal in mucus evasion. There was

no significant difference between the single and double neuraminidase mutants, consistent with the observation that NanB is required for *nanA expression*.

Next, to quantify Spn removal of sialic acid from mucus, we developed a sensitive ELISA to detect removal of sialic acid. In this ELISA, hNF was immobilized and following incubation with bacteria, sialic acid removal was quantified through binding of a lectin specific for α-2,3-linked sialic acid. We observed loss of lectin binding with the parent strain, which correlated with the presence neuraminidases (Fig. 5B). In contrast, lectin binding was maintained following incubation with either single or the double neuraminidase mutants, demonstrating an inability to removal sialic acid due to the lack of neuraminidase enzymatic activity. No difference in the ability of the single mutants and double neuraminidase mutants or the enzymatically-inactive $NanB_{D270A}$ point mutant to remove α-2,3-linked sialic acid was again consistent with our observation that the NanB neuraminidase activity regulates *nanA* expression. The total absence of neuraminidase activity in the *nanA*-deficient strain, when *nanB* is still expressed, also suggested that NanB does not contribute to the bulk of mucus desialylation independently of its effects on *nanA* expression.

Effect of Spn neuraminidases in murine colonization

To determine whether the neuraminidases impact colonization fitness, we measured URT colonization density using an adult mouse model. We continued to use the Type 23F::pilus-1 strain to correlate with our *in vitro* studies, as the presence of the pilus locus has no impact on murine colonization (5). As a sensitive measure of the contribution of these genes *in vivo*, we looked at the competitive index of the parent

strain compared to the double mutant, focusing on early timepoints when Spn is seen predominantly associated with luminal mucus (Fig. 6A) (2). The double neuraminidase mutant significantly outcompeted its parent strain at 4 and 24 hr post-infection, although this increased retention of the double mutant soon after inoculation was relatively modest. This observation indicated a temporary advantage to the increased mucus-binding phenotype of the mutant. When the strains were tested individually, no difference in colonization levels was detected at 4 or 24 hr (Fig. 6B). In infant mice, which are more susceptible to Spn infection, there was also difference in colonization at 5 days post-challenge. As we only observed the contribution of the neuraminidases in a competitive infection, when the wild-type strain could be complementing the mutant; this suggested the possibility of additional effects of the neuraminidase locus.

Spn stimulates mucus containing secretions *in vivo* in a neuraminidase-dependent manner

To more fully understand the impact of neuraminidases on mucosal interactions, we examined URT tissue sections at day 5 post-infection comparing the wild-type strain and Δ*nanA, nanB*::janus mutant. Similar numbers of pneumococci were seen along the mucosal surfaces, consistent with measurement of the colonization density at this time point (Fig. 7A, upper row). Using a lectin that detects α-2,6 linked sialic acid, we observed increased levels of staining of the respiratory epithelium when infected with wild-type Spn, that was reduced in the double neuraminidase mutant, with the latter resembling the mock-infected group (Fig. 7A, upper row). These observations were counter-intuitive since the wild-type strain cleaves sialic acid, but more sialic acid was

311 detected than in mock-infected animals. This raised the possibility that infection with the
312 wild-type strain was inducing more mucus containing secretions. Accordingly, a thicker
313 glycocalx layer and increased staining in glandular structures along the mucosa in wild-
314 type colonized mice was seen by alcian blue-PAS staining for mucopolysaccharides
315 relative to mock-infected controls (Fig. 7A, lower row). To quantify the results, we
316 compared sialic acid levels and amounts of mucus in immunoblots of mNLs using a
317 sialic acid binding lectin and a mAb to the Muc5AC mucin (Fig. 7B, C). We observed a
318 significant increase in sialic acid- and mucin-containing secretions in wild-type
319 compared to both the Δ*nanA, nanB*::janus mutant and mock-infected animals. When we
320 compared the single neuraminidases mutants to wild-type, we observed that in both
321 tissues sections staining for sialic acid or mucopolysaccharides and immunoblots of
322 mNLs to quantify sialic acid or mucin, the *nanA* and *nanB* mutants showed a staining
323 pattern similar to the double neuraminidase-deficient strain (Fig. 7 A, B,C). Together,
324 these results demonstrated that during URT colonization, Spn stimulates sialic acid
325 containing secretions in a neuraminidase dependent-manner and that both
326 neuraminidases are required for these effects.
327
328 **Discussion:**
329 The interactions of a mucosal pathogen with host mucus were examined in this
330 study. The investigation of mucosal pathogens has focused on interactions with
331 epithelial cells even though organism's such as Spn are often found in embedded in the
332 mucus layer during colonization. Mucus is especially challenging to incorporate in *in*
333 *vitro* studies because of its marked heterogeneity, insoluble components and its viscous

334 nature. Many studies have dealt with these limitations through the use of purified or
335 semi-purified mucins, rather than native mucus. An additional challenge in using human
336 mucus with human commensals/pathogens is the immunological components such as
337 S-IgA that associates with mucus (5). Our studies used lavages of the murine URT as a
338 source of mucus so that our findings could be correlated *in vivo* using murine models of
339 colonization or hNF, collected and pooled from multiple donors, as a source of mucus
340 from the natural niche of Spn. We took a broad view to interrogate Spn interaction with
341 mucus by focusing on Spn surface factors. The capsule served as a positive control to
342 validate our adherence assays (16). Among the surface factors tested that had
343 previously been implicated in mucus interactions, there was no role of a putative mucin
344 binding protein MucBP or, in the absence of specific S-IgA using mucus from murine
345 lavages, the Type 1 pilus (24,5). We observed that Spn surface enzymes modify mucus
346 to reduce bacterial adherence and that the major pneumococcal factors involved are the
347 neuraminidases. Decreased mucus binding can be explained by a reduction in the
348 anionic and hydrophobic characteristics of mucus glycoconjugates through removal of
349 terminal sialic acid residues or removal of residues to which Spn can bind. There were
350 inconsistent effects with other exoglycosidases (StrH and BgaA), suggesting that the
351 main mechanism affecting mucus interactions with Spn is through desialylation rather
352 than further deglycosylation once terminal sialic acid is removed. EstA is reported to
353 improve the efficiency of neuraminidases by deacetylation of sialic acid residues in a
354 host species-dependent manner, but we were unable to confirm its role in the observed
355 neuraminidase-dependent effects in our experimental approach (8).

356 It was unexpected that knocking out either *nanA* or *nanB* would increase mucus
357 adherence and eliminate mucus desialylation and neuraminidase activity. This raised
358 the question why Spn expresses two neuraminidases that function in in a non-
359 redundant and non-additive manner. NanA has been established in the literature as a
360 typical hydrolytic sialidase that cleaves *α* 2,3-, *α* 2,6- and *α* 2,8-linked sialic acids to
361 produce *N*-acetylneuraminic acid and as a Spn virulence factor (21,31). In contrast, a
362 distinct role of NanB in the pathogenesis of Spn infection has been less clear. NanB has
363 been reported to be an intramolecular trans-sialidase that acts to preferentially cleave α
364 2,3-linked sialic acid substrates to release 2,7-anhydro-Neu5Ac and has been shown to
365 function in the deglycosylation of host glycoconjugates (29,30). Both neuraminidases
366 contain N-terminal signal sequences and are secreted enzymes. NanA, however, is cell
367 wall-associated due to a typical C-terminal sortase-dependent anchoring motif, which is
368 absent in NanB (32, 21,33). The lower neuraminidase activity observed in the Type 4
369 (TIGR4) strain could be due to the truncation in the LPxTG, eliminating cell-wall
370 anchoring by sortase. Using an outbred mouse model of infection, both NanA and NanB
371 have been shown to be essential for colonization and infection of the upper and lower
372 respiratory tract and for survival in the blood (31,47). However, in previous studies from
373 our lab using infant rat models, NanA was shown to have no role in colonization (37).
374 Based on our findings, we propose the following model. Spn's upregulation of
375 *nanA* expression requires sensing of host-derived sialic acid but this enzyme is surface
376 associated and free sialic acid is not readily available in its URT microniche (14). To
377 provide a source of sialic acid, it must be liberated from host glycoconjugates and this
378 requires a secreted neuraminidase, NanB, encoded on a separate operon, *nan* II (23).

(Some strains also encode for NanC, which has many features in common with NanB). 2,7-anhydo-Neu5Ac released by NanB is internalized through an ABC transporter (SPD_1493-SPD_1495) also encoded by the *nan* II operon, as has been suggested for homologs in another bacterial species, *Ruminococcus gnavus* (34). Once inside the cell, an oxidoreductase (SPD_1498) and a putative isomerase (SPD_1503), also encoded by *nan* II, covert 2,7-anhydo-Neu5Ac to Neu5Ac, again suggested by the role of a homologous oxidoreductase in *R. gnavus* (34). The *nan* II operon, therefore, appears to function to liberate a source of sialic acid derived from host glycoconjugates to be taken up and sensed within the bacterial cell. Unlike other genes in the *nan* locus, the *nan* II operon is not regulated by *nanR*, which appears to act downstream on the other transcriptional units of the *nan* locus (23). Internalized sialic acid produced by the combined activity of NanB and the other genes in the *nan* II operon might modify transcription control of *nanA* through its activator NanR. Since NanB does not influence the transcription of *nanR*, the regulator of *nanA*, this suggests that NanB-dependent transcriptional control of *nanA* is post-transcriptional with respect to *nanR* expression (Fig. 4E). NanA is the main functional Spn neuraminidase as in its absence *nanB* is still expressed but there was no detectible evasion of mucus binding or desialylation of mucus. Thus, this report assigns a mechanistic role to 'the second neuraminidase' of Spn, NanB, and puts into perspective why prior studies were unable to account for its function apart from that of NanA.

Previous *in vivo* studies examining the contribution of Spn's neuraminidases have yielded mixed results (31, 6, 35, 37). The lack of a colonization defect for the Δ*nanA,nanB*::janus mutant was surprising considering its robust mucus adherence

phenotype. Interactions with mucus, however, are likely to be complex. The first encounter of Spn with its host is with 'loose' luminal mucus (2). Our finding that the neuraminidase-deficient mutant shows an early competitive advantage suggests that attaching to this material might aid in retention of the bacterial inoculum. However, during the period of stable colonization (>24hrs p.i.), when Spn has migrated to the glycocalyx, we confirmed that the presence of Spn increases URT secretions, a result that recapitulates the correlation between rhinitis symptoms and Spn carriage in young children (41,42). Adults, who have a lower density of colonizing Spn, have less pronounced secretions during episodes of carriage. In infant mice, increased secretions in URT lavages and along the mucosa (see as a thicker glycocalyx layer) depended on the expression of its neuraminidases with deletion of either eliminating this effect as NanB controls expression of *nanA*. The neuraminidase-mediated increase in URT secretions was independent any effects of the neuraminidases on levels of Spn colonization. It appears, therefore, that the neuraminidase-mediated stimulation of mucus which could otherwise sweep away colonizing pneumococci is balanced by modulation of mucus by neuraminidases to limit bacterial binding and removal by mucociliary clearance. It remains unclear how bacterial neuraminidase acts on the mucosa to increase mucus production and flow. Since neuraminidases mediate both an effect on mucus production and evasion it is difficult to test conditions to that could distinguish these effects. Interestingly, influenza virus, which contains a neuraminidase, induces copious mucus production in the URT(14,41). In the setting of influenza A co-infection, the neuraminidase-deficient Spn mutant has been shown to exhibit decreased levels of colonization compared to controls without influenza A co-infection(14,48). We

postulate that this is due to the inability of the mutant to evade mucus binding when mucus secretions are abundant, although we cannot exclude other effects of neuraminidases such as providing a source of sialic acid for nutritional purposes. (39,40). Additionally, in previous TnSeq screens of Spn genes affecting mouse colonization, we and others observed selection against *nanB* (P=0.01) and *nanA* (P=0.029) mutants (43,44). This could be explained by the decreased mucus evasion of these mutants under conditions where mucus production is stimulated by co-colonizing strains still expressing neuraminidase. A further consideration is that Spn may need to fine tune mucus production and binding to allow it to be shed from its host in URT secretions in the process of transmission to a new host.

In summary, by studying Spn-mucus interactions we found that Spn expresses at least two neuraminidases because one is required for the expression of the other – an unusual scenario where an organism's ability to target a host substrate depends on an enzyme with related function. In particular, our findings show that the Spn neuraminidases act together to desialylate mucus to limit bacterial binding. We postulate that during colonization neuraminidase-dependent reduction in mucus binding facilitates evasion of mucociliary clearance which is needed to counter neuraminidase-mediated stimulation of mucus secretions.

Materials and Methods

Ethics Statement

All animal experiments followed the guidelines summarized by the National Science Foundation Animal Welfare Act (AWA) and the Public Health Service Policy on the

Humane Care and Use of Laboratory Animals. The Institutional Animal Care and Use Committee (IACUC) at New York University School of Medicine oversees the welfare, well-being, proper care and use of all animals, and they have approved all the protocols used in this study.

Mice

C57BL/6J mice were purchased from The Jackson Laboratory (Bar Harbor, ME), and were bred and housed in a conventional animal facility. Throughout all experiments, the mice were healthy and did not lose weight compared to uninfected controls.

Chemicals and reagents

Bovine serum albumin (BSA; A9430), sodium periodate (Cat. No. 71859), O-phenylenediamine dihydrochloride (Cat. No. P9187), cholera filtrate lyophilized powder (Cat. No. C8772), mutanolysin (Cat. No. M9901), lysozyme (L6876), Tween 20 (Cat. No. P9416), Trypsin (Cat. No. 85450C) and Alcian blue solution (Cat. No. B8438) were obtained from Millipore Sigma (Darmstadt, Germany). Rabbit anti-pneumococcus Type 4 serum (Cat. No. 16747) and Type 23F serum (Cat. No. 16913) were obtained from Statens Serum Institut (Copenhagen, Denmark). Triton X-100 (9002-93-1) was obtained from Amresco (Solon, OH, USA). HRP-coupled streptavidin (Cat. No. 21130), 4% paraformaldehyde solution (Cat. No. AAJ19943K2), NA-STAR kit to assay neuraminidase activity (Cat. No. 4374422), High-Capacity cDNA Reverse Transcription Kit (Cat. Not. 4368814), Power SYBR Green PCR Master Mix (Cat. No. 4374967), 2X Phusion Master Mix (Cat. No. F531L), and Dulbecco′s Modified-Eagle′s Medium

(DMEM, Cat. No. 11995-065) were obtained from Thermo Fisher Scientific (Waltham, MA, USA). FITC-conjugated mouse anti-goat antibody (Cat. No. sc-2356) was purchased from Santa Cruz (Dallas. TX, USA). Bradford Reagent (Cat. No. 500-0006) was obtained from Bio-Rad (Hercules, CA, USA). Biotinylated Maackia Amurensis Lectin II (MAL II, B-1265), Biotinylated Sambucus Nigra Lectin (SNL, EBL, B-1305), Biotinylated Maackia Amurensis Lectin I (MAL I, B-1315), and Carbo-Free blocking agent (Cat. No. SP-5040) were purchased from Vector Laboratories (Burlingame, CA, USA). Biotin-labelled Mucin 5AB-1 (45M1) was purchased from NeoMarkers Inc. (Portsmouth, NH, USA). RNAprotect cell reagent (Cat. No. 76526) and RNeasy (Cat No./ID: 74106) were obtained from Qiagen (Hilden, Germany). MasterPure DNA purification kit (Cat. No. MCD85201) was obtained from Epicentre (Middleton, WI, USA). GoTaq Green Master Mix (Cat. No. M7123) was obtained from Promega (Madison, WI, US).

Bacterial culture

The Type 4 (T4) and Type 23F (T23F) *Streptococcus pneumoniae* (Spn) strains that were used in this study are listed in Table 1. Spn were grown on tryptic soy (TS; Becton Dickinson) agar plates supplemented with 100 µl of catalase (30,000 U/ml; Worthington Biomedical) and appropriate antibiotics (200 µg/ml streptomycin, str; 125 or 250 µg/ml kanamycin, kan; 2 µg/ml chloramphenicol, 1 µg/ml erythromycin, or 200 µg/ml spectinomycin), overnight at 37°C and 5% CO_2. The Spn CFU/mL was confirmed for each assay described below by plating serial dilutions on TS agar (supplemented with the appropriate antibiotic). Broth-grown Spn were obtained by static culture in TS broth

494 at 37°C to an OD_{620} of 1.0 or 0.6 for *in vivo* and *in vitro* experiments, respectively,
495 unless otherwise specified. Spn were centrifuged at 10,000xg for 1 min, washed, and
496 diluted in sterile PBS to the desired concentration.
497
498 **Bacterial strain construction**
499 The primers used to construct all of the bacterial strains are listed in Table S2.
500 The in-frame and unmarked deletion pneumococcal strains, deficient for the genes
501 *nanA, nanB, mucBP, estA,* and *strH,* were constructed in a two-step process using the
502 Janus cassette (19). First, genomic DNA from strain P2408, containing the Janus
503 cassette, was isolated using the MasterPure DNA purification kit (MCD85201 Epicentre,
504 Middleton, WI, USA). For constructing *nanB*-deletion mutants, flanking regions 1 kb
505 upstream and downstream of the Spn *nanB* gene were added to the Janus cassette via
506 isothermal assembly (using primers 83F and 84R, 85F and 86R, and 87F and 88R)
507 (27). The PCR product was then transformed into the str^R T4 parent strain Spn P2406
508 and the transformants were selected on TS-kan (250 µg/ml) plates. The presence of the
509 Janus in the *nanB* gene in P2406 was confirmed by PCR (GO-Taq polymerase,
510 Promega M7123, and primers 83F and 88R). A second PCR amplicon was generated
511 by amplifying and joining the upstream and downstream regions around *nanB* from Spn
512 P2406 (using primers 1F and 2R and primers 3F and 4R). Spn P2613, the intermediate
513 strain (*nanB*::Janus; kan^R, str^S), was transformed with this PCR product to generate an
514 in-frame, unmarked *nanB* deletion strain. Transformants were selected on TS-str to
515 generate strain P2619 (Δ*nanB*; str^R, kan^S) and was confirmed by PCR (GO-Taq
516 polymerase using primers 83F and 88R). The in-frame knockout strain P2619 has a

517 scar containing the first and the last 5-amino-acid coding sequences of the *nanB* gene.
518 The *nanB* corrected strain P2623 (Δ*nanB*::*nanB*; str^R, kan^S), was constructed by
519 transforming P2613 (*nanB*::Janus*)* with a complete *nanB* PCR product generated using
520 primers 1F and 4R on strain P2406; the transformants were selected on TS-str. None of
521 the constructed strains showed a growth defect when cultured in TS broth. This same
522 procedure was used to a create in-frame, unmarked deletion strains of *nanB* and the
523 chromosomally corrected mutant in Spn T23F P1121, and *nanA*, *nanB* and their
524 respected chromosomally corrected mutants in the previously-described Spn Type
525 23F::pilus-1 P2588 strain (18,5). The Spn strains that were generated in this study are
526 listed in Table S1.
527 To create a Spn strain with an enzymatically-inactive NanB, a PCR product was
528 generated (using the primer pairs consisting of 79F and 81R and 80F and 82R) to
529 amplify *nanB* from Spn P2499 (a strR derivative of P1121). The primers were
530 constructed to replace an asparagine at amino acid 270 with an alanine. The PCR
531 fragment was transformed into Spn P2637 (Δ*nanB::janus;* str^S, kan^R) and transformants
532 were selected on TS-str (200 ug/ml) and confirmed by PCR (GO-Taq polymerase using
533 primers 1F and 4R). The mutation was validated by Sanger sequencing.
534
535 **Human and mouse nasal fluid binding assays**
536 Pooled nasal secretion samples from six adult volunteers were purchased from
537 LeeBio (Maryland Heights, MO, USA, 991-13-S). Human nasal fluid samples were
538 sonicated on ice (5 seconds at amplitude of 8 um; Fisher Scientific Model 705 Sonic
539 Dismembrator) to create homogenous samples. Murine nasal lavages (mNL) were

collected from uninfected, adult C57BL/6J mice through post-mortem retro-tracheal lavages with 400uL sterile PBS (pH 7.4) and pooled.

Adherence of different pneumococcal strains to hNF or mNL was assessed in a solid phase-binding assay as previously described (5). Briefly, 100uL of hNF (10ug/100uL in PBS) or mNL (undiluted) were immobilized on a 96-well flat-bottom polystyrene plate (Sarstedt REF:82.1581.001) by centrifugation (250 x g for 3min, RT) and incubated overnight at 37°C in 5% CO_2. Wells were then washed 3 times with 100uL of DMEM and blocked with 0.1% BSA-DMEM for 2h at RT. The wells were then washed 3 times with 100uL of DMEM and Spn (2×10^4 CFU/mL in 100uL of DMEM, grown to mid-log phase (OD_{620}= 0.6) in TS broth and then diluted to the desired concentration) were added to each well. The plate was then centrifuged (250 x g, 3min, RT) and the plate was incubated at 30°C and 5% CO_2 for 2h to allow the Spn to bind. Then, to remove unbound bacteria, the wells were gently washed 19 times with 100uL of DMEM. Adherent bacteria were collected by adding 100 µl of 0.001% Triton X100-PBS and incubating for 15 min at RT followed by vigorous mixing. To quantify the adherent bacteria, samples were plated in triplicate on TS agar plates with select antibiotics and incubated overnight at 37°C with 5% CO_2. Each experimental condition was assayed in triplicate for each experiment.

In some assays, mNL was modified after immobilization. To assess the role of carbohydrate oxidation, immobilized mNL was pretreated for 30 minutes with 100uL of 100mM of sodium periodate ($NaIO_4$, Sigma, Cat. No. 71859) in 50mM sodium acetate buffer (pH 4.5) and then blocked with 0.1% BSA-DMEM for 2h at RT. The high concentration of NaIO4 (100mM) provides non-specific oxidation of sugar moieties (38).

563 To assess the role of protein cleavage, immobilized mNLs were treated with 50µg/ml
564 trypsin (Sigma, Cat. No. 85450C) in 100uL PBS and then blocked with 0.1% BSA-
565 DMEM for 2h at RT.

566 For neuraminidase complementation studies, immobilized hNF were pretreated
567 with 200uL cholera filtrate (a source of neuraminidase, Sigma Aldrich, C8772)
568 resuspended in calcium saline solution at 100 U/mL and incubated overnight at 37°C
569 and 5% CO_2. The wells were then washed 3 times with 100uL DMEM and blocked with
570 0.1% BSA-DMEM for 2h at RT.

571

572 **Sialic Acid Quantification ELISA**

573 An ELISA was used to measure the removal of hNF sialic acid by Spn. Wells of a
574 microtiter plate (96-well, Immulon 4HBX plate, Thermo Fisher Scientific) were coated
575 with 100uL hNF (10ug/100uL) diluted in PBS (pH 7.4) and incubated overnight at 37°C
576 and 5% CO_2. The wells were washed 3 times with 100uL DMEM, and blocked with
577 200uL of Carbo-Free Blocking Solution (Vector Laboratories, SP-5040) for 2h at RT.
578 The wells were washed 3 times with 100uL of DMEM. Bacteria (100uL of 5 x 10^6
579 CFU/mL Spn grown to mid-log phase (OD_{620}= 0.6) and diluted to the desired
580 concentration in DMEM) were added to the wells and the plate was incubated for 4h at
581 30°C and 5% CO_2. The wells were then gently washed 19 times with 100uL of washing
582 buffer TPBS (PBS + 0.01% Tween 20). Remaining -2,3-linked sialic acid was detected
583 by adding 100uL biotin-linked Mal II (2.5ug/mL; Vector Laboratories, B-1265) and
584 incubating for 1h at RT. Wells were washed 3 times with 100uL PBS and incubated with
585 streptavidin-horseradish peroxidase (HRP)-conjugate (Pierce #21130) diluted 1:5,000 in

PBS for 1h at RT. Wells were washed three times with 100uL PBS; O-phenylenediamine dihydrochloride (Sigma, P9187) was used as an HRP substrate, according to manufacturer's directions. The color reaction was measured at an absorbance of 492 nm using a SpectraMax M3 plate reader (Molecular Devices). The absorbance of the PBS control wells were averaged and the value was subtracted from each measured experimental value.

Microscopy

For microscopic visualization of mNLs and hNF, nasal fluid samples were processed and assessed as previously described (5). Briefly, 1µL of 5 x 10^4 CFU/mL Spn were incubated with 10 µl of undiluted hNF or mNL for 2 h at 37°C and 5% CO_2. The total volume of sample (11µL) was then placed onto glass slides and heat fixed by flame. To visualize mucus, samples were incubated with 3% acetic acid for 5 min and followed by Alcian blue (Sigma, B8438) (in 3% acetic acid, pH 2.5) for 30 min. After washing the samples in sterile water for 10 min, slides were blocked in 10% fetal bovine serum (FBS; Peak Serum PS-FB1) in PBS at 4°C overnight. Bacteria were stained with rabbit anti-capsule (Type 4 (Statens Serum Institut, 16747) and Type 23F serum (Statens Serum Institut, 16913) antibody (1:200 in 0.5% FBS-PBS) and secondary goat anti-rabbit IgG-FITC (1:100 in 0.5% FBS-PBS) (Santa Cruz, Cat. No. sc-2356). Spn were visualized on an Axiovert 40 CFL microscope with an Axiocam IC digital camera (Zeiss). Images were analyzed with ZEN 2012 software and, for brightness and contrast, processed with ImageJ 1.52a software.

609 **Neuraminidase activity assay**

610 To determine the neuraminidase activity for the Spn strains, we used the NA-
611 STAR kit from Thermo-Fischer (4374422) according to the manufacturer's protocol. In
612 summary, bacteria were grown to an OD_{620} =1.0, centrifuged at 10,000 x *g* for 1min and
613 resuspended in 250uL of PBS to a density of 10^7 CFU/mL. Bacterial suspensions were
614 sonicated on ice (15s on, 45s off for 8 min total; amplitude 8 um; Fisher Scientific Model
615 705 Sonic Dismembrator). The samples were centrifuged at 10,000 x *g* for 1 min, and
616 the supernatant was kept on ice until neuraminidase activity was assayed. Using the
617 plates from the NA-STAR kit, 25uL of NA-Star assay buffer was added to both bacterial
618 and control wells. Next, 50uL of PBS was added to the control wells and 50uL of sample
619 was added to the bacterial wells. The plate was incubated for 20 minutes at 37°C and
620 5% CO_2. 10uL of diluted NA-STAR substrate in NA-STAR buffer was added to each
621 well and the plate was incubated for 30 minutes at RT. To assess the chemiluminescent
622 signal, 60uL of NA-STAR accelerator was added to each well and the chemiluminescent
623 signal (Luminescence program, check LM1 all) was read by a SpectraMax M3 reader
624 (Molecular Devices). To analyze the data, the "signal" (luminescence value for each
625 sample) was divided by the "noise" (luminescence value of PBS control wells).

626 The presence of sialic acid in mNL on neuraminidase activity of Spn strains was
627 assessed as follows. Briefly, starting at an OD_{620}=0.2, Spn were grown in TS broth for
628 45 minutes; 3 mL of culture was then centrifuged at 10,000x*g* for 1 min, and the pellet
629 was resuspended in 3mL DMEM. The bacteria were diluted 1:50 into 3mL DMEM alone,
630 or into 3mL DMEM with 140uL of mNL. The samples were incubated for 3 h at 37°C

631 with 5% CO_2. The samples were then centrifuged at 10,000 x g for 1 min, resuspended
632 in 250uL PBS, and neuraminidase activity assayed as described above.
633
634 **Quantitative RT-PCR**
635 Spn were grown in TS broth to an OD_{620}= 1.0. Samples were mixed with an
636 equal volume of RNA protect (Qiagen, 76526) and incubated for 5 min at RT followed
637 by centrifugation for 1 min at 10,000 x g; the bacterial pellet was stored at -80°C. To
638 extract RNA, Spn pellets were thawed and treated with 27uL mutanolysin (200 mg/mL,
639 Sigma M9901), 18uL Proteinase K (20 mg/ml, Denville Scientific CB3210-5), 27uL of
640 lysozyme (100 mg/mL, Sigma L6876), and 128uL of TE buffer (10mM TrisCl, 1mM
641 EDTA, pH 8.0, nuclease-free water) for 20 min at RT. RNA extraction (RNeasy, Qiagen)
642 and subsequent cDNA generation (High Capacity cDNA Reverse Transcriptase Kit,
643 Applied Biosystems, Thermo Fisher Scientific), were performed according to
644 manufacturer's instructions. PCR with *gapdh* was performed on purified RNA to check
645 for DNA contamination. qRT-PCR. Reaction samples contained ~10ng cDNA and 0.5
646 µM primers in Power SYBR Green PCR Master Mix (Applied Biosystems, Thermo
647 Fisher Scientific) and samples were tested in duplicate. qRT-PCR reactions were run in
648 a 384 well plate (Bio-Rad) using CFX384 Real-Time System (Bio-Rad). Expression
649 of *16S* and *gapdh* were normalization controls and fold-change in gene expression was
650 quantified according to the ΔΔCt method (36). The primer sequences used in this assay
651 are indicated in Table S3.
652 **Mouse Infections**

Spn strains were grown in TS broth to an OD_{620}=1, washed, and diluted to the desired density in sterile PBS. Six-week old adult mice were infected intranasally without anesthesia, with 10uL containing ~1-2 x 10^5 CFU of either Spn strain P2588 (Type 23F, Δ *pilus-1)* or P2636, the isogenic neuraminidase-deficient strain (Type 23F, Δpilus-1, Δ*nanA*, Δ*nanB::Janus*) alone, or with an inoculum containing a 1:1 ratio of P2588 and P2636. Four-day old mice were infected intranasally without anesthesia, with 3uL containing 1-2x 10^3 CFU of either Spn strain P2588 or P2636. At 4h, 24h, and 5 days post-pneumococcal challenge, mice were euthanized with CO_2 followed by cardiac puncture. For quantification of URT colonization density, the trachea was cannulated and lavaged with 200uL sterile PBS, and fluid was collected from the nares. The nasal lavage samples were plated in serial dilutions on TS-str or TS-kan (250ug/mL) plates and incubated overnight at 37 °C with 5% CO_2.

Immunoblot

An immunoblot of mNL obtained from Spn-colonized mice provided a quantitative assessment of α-2,3-linked sialic acid or MUC5AC levels. Four-day old pups were infected with P2588 (Type 23F:: pilus-1*)*, P2636 (Type 23F:: pilus-1, Δ*nanA*, *nanB::*janus), P2634 (Type 23F:: pilus-1, Δpilus-1, Δ*nanA*), P2637(Type 23F:: pilus-1, *nanB::*janus), P2642 (Type 23F:: pilus-1, $NanB_{D270A}$) as described above, or mock-infected with PBS as a control. URT lavages were obtained 5d p.i.,and stored at -20°C until use. mNL were diluted 1:5 in PBS and 100uL was applied to a 0.2-µm nitrocellulose membrane (Amersham Protran 0.2µm GE10600094) with vacuum using a Minifold II Slot- Blot apparatus (Schleicher & Schuell). Air dried membranes were

676 incubated in 2% BSA-Tris-buffered saline (TBS) at 4°C overnight with shaking. The
677 membrane was incubated for 1h at RT in 2ug/mL Maackia Amurensis Lectin I
678 biotinylated (Vector Laboratories #B-1315) or 1:500 of MUC5AC monoclonal antibody
679 (NeoMarkers #45M1) diluted in TBS. The blot was washed 6 times (5 minutes each
680 wash) with 0.1% Tween-20-TBS, and incubated for 1h at RT with streptavidin-
681 horseradish peroxidase (HRP)-conjugate (Pierce #21130) diluted 1:100,000 in TBS.
682 The membrane was washed once for 1.5 hr, followed by 5 times (15 minutes each
683 wash) with 0.1% Tween-20-TBS and was developed, according to manufacturer's
684 directions, with the Super Signal West Femto substrate (Thermo Scientific Cat. No.
685 34095). The chemiluminescent signal was visualized using the iBright CL1000 imaging
686 system (Thermo Fisher Scientific) and the relative intensities of the bands on the
687 membrane were quantified through assessing integrated pixel density.

688 **Histopathology**

689 Pups were euthanized as per standard protocol. Skin of heads were gently removed
690 with caution to preserve nasal structures. Heads were then decapitated and submerged
691 in PBS at 4°C for a brief wash, followed by fixing in 4% paraformaldehyde for 48-72 hrs
692 at 4°C without shaking. Heads were then washed in PBS at 4°C with gentle swirling x
693 20 minutes, followed by decalcification by fully submerging heads into 0.12M EDTA
694 solution at 4°C with gentle shaking for 7 days. Intact heads were then processed
695 through graded ethanols to xylene and infiltrated with paraffin in a Leica Peloris
696 automated tissue processor. Five um paraffin-embedded sections were stained either
697 with PAS and alcian blue (Freida L Carson, Histotechnology 2nd Ed., 1997) or with lectin
698 and antibody probes on a Leica BondRX automated stainer, according to the
699 manufacturer's instructions. In brief, sections were incubated for 2 hours with SNL-EBL
700 conjugated to Cy5 (1:50 dilution, Vector Labs, cat # CL-1303) followed by 1 hour with

Spn typing sera (1:2000 dilution, SSI diagnostica, cat # 16913) and then 1 hour with goat-anti rabbit IgG conjugated to Alexa Fluor 594 (1:100, ThermoFisher A21207). Slides were scanned on an Akoya Polaris Vectra imaging system. The multispectral images were unmixed and autofluorescence signal removed with the Akoya InForm software prior to exporting as tif files.

Statistical analysis

GraphPad Prism (version 7.01, San Diego, CA) was used for statistical analysis. A t-test or one-way ANOVA, with either Sidak's or Dunnett's multiple comparison test, was performed unless otherwise noted.

Acknowledgements

We would like to thank the NYU Experimental Pathology Research Laboratory for assisting with the histopathology studies. The core is partially supported by the Cancer Center Support Grant P30CA016087 at NYU Langone's Laura and Isaac Perlmutter Cancer Center and the Vectra Imaging system was awarded as Shared Instrumentation Grant S10 OD021747 grant.

This study was supported by grant from the National Institute of Health to J.N. Weiser (R37 AI038446, R21 AI50867, R01 AI50893).

References

1. Weiser JN, Ferreira DM, Paton JC. Streptococcus pneumoniae: transmission, colonization and invasion. Nat Rev Microbiol. 2018;16(6):355-67.
2. Nelson AL, Roche AM, Gould JM, Chim K, Ratner AJ, Weiser JN. Capsule enhances pneumococcal colonization by limiting mucus-mediated clearance. Infect Immun. 2007;75(1):83-90.
3. Cone RA. Barrier properties of mucus. Adv Drug Deliv Rev. 2009;61(2):75-85.
4. Wagner CE, Turner BS, Rubinstein M, McKinley GH, Ribbeck K. A Rheological Study of the Association and Dynamics of MUC5AC Gels. Biomacromolecules. 2017;18(11):3654-64.
5. Binsker U, Lees JA, Hammond AJ, Weiser JN. Immune exclusion by naturally acquired secretory IgA against pneumococcal pilus-1. J Clin Invest. 2020;130(2):927-41.
6. King SJ, Hippe KR, Weiser JN. Deglycosylation of human glycoconjugates by the sequential activities of exoglycosidases expressed by Streptococcus pneumoniae. Mol Microbiol. 2006;59(3):961-74.
7. Taherali F, Varum F, Basit AW. A slippery slope: On the origin, role and physiology of mucus. Adv Drug Deliv Rev. 2018;124:16-33.
8. Kahya HF, Andrew PW, Yesilkaya H. Deacetylation of sialic acid by esterases potentiates pneumococcal neuraminidase activity for mucin utilization, colonization and virulence. PLoS Pathog. 2017;13(3):e1006263.
9. Pettigrew MM, Fennie KP, York MP, Daniels J, Ghaffar F. Variation in the presence of neuraminidase genes among Streptococcus pneumoniae isolates with identical sequence types. Infect Immun. 2006;74(6):3360-5.
10. Xu G, Kiefel MJ, Wilson JC, Andrew PW, Oggioni MR, Taylor GL. Three Streptococcus pneumoniae sialidases: three different products. J Am Chem Soc. 2011;133(6):1718-21.
11. Walther E, Richter M, Xu Z, Kramer C, von Grafenstein S, Kirchmair J, et al. Antipneumococcal activity of neuraminidase inhibiting artocarpin. Int J Med Microbiol. 2015;305(3):289-97.
12. Brittan JL, Buckeridge TJ, Finn A, Kadioglu A, Jenkinson HF. Pneumococcal neuraminidase A: an essential upper airway colonization factor for Streptococcus pneumoniae. Mol Oral Microbiol. 2012;27(4):270-83.
13. Marion C, Burnaugh AM, Woodiga SA, King SJ. Sialic acid transport contributes to pneumococcal colonization. Infect Immun. 2011;79(3):1262-9.
14. Siegel SJ, Roche AM, Weiser JN. Influenza promotes pneumococcal growth during coinfection by providing host sialylated substrates as a nutrient source. Cell Host Microbe. 2014;16(1):55-67.
15. Ankur B. Dalia AJS, Jeffrey N. Weiser Three Surface Exoglycosidases from Streptococcus pneumoniae, NanA, BgaA, and StrH, Promote Resistance to Opsonophagocytic Killing by Human Neutrophils. Infection and Immunity. 2018;78 (5):2108-16.
16. Zafar MA, Hamaguchi S, Zangari T, Cammer M, Weiser JN. Capsule Type and Amount Affect Shedding and Transmission of Streptococcus pneumoniae. mBio. 2017;8(4).

17. Zafar MA, Kono M, Wang Y, Zangari T, Weiser JN. Infant Mouse Model for the Study of Shedding and Transmission during Streptococcus pneumoniae Monoinfection. Infect Immun. 2016;84(9):2714-22.

18. Shen P, Lees JA, Bee GCW, Brown SP, Weiser JN. Pneumococcal quorum sensing drives an asymmetric owner-intruder competitive strategy during carriage via the competence regulon. Nat Microbiol. 2019;4(1):198-208.

19. Sung CK, Li H, Claverys JP, Morrison DA. An rpsL cassette, janus, for gene replacement through negative selection in Streptococcus pneumoniae. Appl Environ Microbiol. 2001;67(11):5190-6.

20. Tettelin, H., K. E. Nelson, I. T. Paulsen, J. A. Eisen, T. D. Read, S. Peterson, J. Heidelberg, R. T. DeBoy, D. H. Haft, R. J. Dodson, A. S. Durkin, M. Gwinn, J. F. Kolonay, W. C. Nelson, J. D. Peterson, L. A. Umayam, O. White, S. L. Salzberg, M. R. Lewis, D. Radune, E. Holtzapple, H. Khouri, A. M. Wolf, T. R. Utterback, C. L. Hansen, L. A. McDonald, T. V. Feldblyum, S. Angiuoli, T. Dickinson, E. K. Hickey, I. E. Holt, B. J. Loftus, F. Yang, H. O. Smith, J. C. Venter, B. A. Dougherty, D. A. Morrison, S. K. Hollingshead, and C. M. Fraser. Complete Genome Sequence of a Virulent Isolate of *Streptococcus pneumoniae*. Science. 2001; 293:498–506

21. Xu G, Potter JA, Russell RJ, Oggioni MR, Andrew PW, Taylor GL. Crystal structure of the NanB sialidase from Streptococcus pneumoniae. J Mol Biol. 2008;384(2):436-49.

22. Rodriguez JL, Dalia AB, Weiser JN. Increased chain length promotes pneumococcal adherence and colonization. Infect Immun. 2012;80(10):3454-9.

23. Afzal M, Shafeeq S, Ahmed H, Kuipers OP. Sialic acid-mediated gene expression in Streptococcus pneumoniae and role of NanR as a transcriptional activator of the nan gene cluster. Appl Environ Microbiol. 2015;81(9):3121-31.

24. Bumbaca D, Littlejohn JE, Nayakanti H, Lucas AH, Rigden DJ, Galperin MY, et al. Genome-based identification and characterization of a putative mucin-binding protein from the surface of Streptococcus pneumoniae. Proteins. 2007;66(3):547-58.

25. Hammerschmidt S, Talay SR, Brandtzaeg P, and Chhatwal GS. SpsA, a novel pneumococcal surface protein with specific binding to secretory Immunoglobulin A and secretory component. *Molecular Microbiology*. 1997; 25(6):1113-24.

26. Ortigoza MB, Blaser SB, Zafar MA, Hammond AJ, Weiser JN, Klugman KP. An Infant Mouse Model of Influenza Virus Transmission Demonstrates the Role of Virus-Specific Shedding, Humoral Immunity, and Sialidase Expression by Colonizing Streptococcus pneumoniae. mBio. 2018;9(6).

27. Lemon JK, Weiser JN. Degradation products of the extracellular pathogen Streptococcus pneumoniae access the cytosol via its pore-forming toxin. mBio. 2015;6(1).

28. Traving, C., Schauer, R. Structure, function and metabolism of sialic acids. CMLS, Cell. Mol. Life Sci. 1998; 54:1330–1349.

29. Xiao K, Wang X, Yu H. Comparative studies of catalytic pathways for Streptococcus pneumoniae sialidases NanA, NanB and NanC. Sci Rep. 2019;9(1):2157.

30. Burnaugh AM, Frantz LJ, King SJ. Growth of Streptococcus pneumoniae on human glycoconjugates is dependent upon the sequential activity of bacterial exoglycosidases. J Bacteriol. 2008;190(1):221-30.

31. Manco S, Hernon F, Yesilkaya H, Paton JC, Andrew PW, Kadioglu A. Pneumococcal neuraminidases A and B both have essential roles during infection of the respiratory tract and sepsis. Infect Immun. 2006;74(7):4014-20.

32. Camara, M., Boulnois, G.J., Andrew, P.W. and Mitchell, T.J. A neuraminidase from Streptococcus pneumoniae has features of a surface protein. Infect Immunity. 1994; 62: 3688–3695.

33. Berry, A.M., Ogunniyi, A.D., Miller, D.C. and Paton, J.C.. Comparative virulence of Streptococcus pneu- moniae strains with insertion-duplication, point, and deletion mutations in the pneumolysin gene. Infect Immunity. 1999; 67: 981–985.

34. Bell A, Severi E, Lee M, Monaco S, Latousakis D, Angulo J, et al. Uncovering a novel molecular mechanism for scavenging sialic acids in bacteria. J Biol Chem. 2020;295(40):13724-36.

35. Orihuela CJ, Gao G, Francis KP, et al. Tissue-specific contributions of pneumococcal virulence factors to pathogenesis. J Infect Dis. 2004;190:1661-1669.

36. Livak KJ, Schmittgen TD. Analysis of relative gene expression data using real-time quantitative PCR and the 2(-Delta Delta C(T)) Method. Methods. 2001;25(4):402-8.

37. King SJ, Hippe KR, Gould JM, Bae D, Peterson S, Cline RT, et al. Phase variable desialylation of host proteins that bind to Streptococcus pneumoniae in vivo and protect the airway. Mol Microbiol. 2004;54(1):159-71.

38. Prakash R, Bharathi Raja S, Devaraj H, Devaraj SN. Up-regulation of MUC2 and IL-1beta expression in human colonic epithelial cells by Shigella and its interaction with mucins. PLoS One. 2011;6(11):e27046.

39. Burnaugh AM, Frantz LJ, King SJ. Growth of Streptococcus pneumoniae on human glycoconjugates is dependent upon the sequential activity of bacterial exoglycosidases. J Bacteriol. 2008;190(1):221-30.

40. Yesilkaya H, Manco S, Kadioglu A, Terra VS, Andrew PW. The ability to utilize mucin affects the regulation of virulence gene expression in Streptococcus pneumoniae. FEMS Microbiol Lett. 2008;278(2):231-5.

41. Zangari T, Ortigoza MB, Lokken-Toyli KL, Weiser JN. Type I interferon signaling is a common factor driving Streptococcus pneumoniae and Influenza A shedding and transmission. mBio. 2020; Under revision.

42. Rodrigues F, Foster D, Nicoli E, Trotter C, Vipond B, Muir P, Gonçalves G, Januário L, Finn A. Relationships between rhinitis symptoms, respiratory viral infections and nasopharyngeal colonization with Streptococcus pneumoniae, Haemophilus influenzae and Staphylococcus aureus in children attending daycare. Pediatr Infect Dis J. 2013;32(3):227-32.

43. Zafar MA, Hammond AJ, Hamaguchi S, Wu W, Kono M, Zhao L, et al. Identification of Pneumococcal Factors Affecting Pneumococcal Shedding Shows that the dlt Locus Promotes Inflammation and Transmission. mBio. 2019;10(3).

44. van Opijnen T, Camilli A. A fine scale phenotype-genotype virulence map of a bacterial pathogen. Genome Res. 2012;22(12):2541-51.

45. Za¨hner, D. & Hakenbeck, R. The Streptococcus pneumoniae b-galactosidase is a surface protein. J Bacteriol, 2000; 182, 5919–5921.

46. Pluvinage B, Chitayat S, Ficko-Blean E, Abbott DW, Kunjachen JM, Grondin J, et al. Conformational analysis of StrH, the surface-attached exo-beta-D-N-acetylglucosaminidase from Streptococcus pneumoniae. J Mol Biol. 2013;425(2):334-49.

47. Janesch P, Rouha H, Badarau A, Stulik L, Mirkina I, Caccamo M, et al. Assessing the function of pneumococcal neuraminidases NanA, NanB and NanC in in vitro and in vivo lung infection models using monoclonal antibodies. Virulence. 2018;9(1):1521-38.

48. Wren JT, Blevins LK, Pang B, Basu Roy A, Oliver MB, Reimche JL, et al. Pneumococcal Neuraminidase A (NanA) Promotes Biofilm Formation and Synergizes with Influenza A Virus in Nasal Colonization and Middle Ear Infection. Infect Immun. 2017;85(4).

49. Shakhnovich EA, King SJ, Weiser JN. Neuraminidase expressed by Streptococcus pneumoniae desialylates the lipopolysaccharide of Neisseria meningitidis and Haemophilus influenzae: a paradigm for interbacterial competition among pathogens of the human respiratory tract. Infect Immun. 2002;70(12):7161-4.

Figure legends:

Figure 1: Mucosal carbohydrate-mediated binding of *S. pneumoniae* to nasal lavages

(A-D) Adherence of Spn Type 4 (TIGR4) to murine nasal lavages (mNL) was analyzed in a solid-phase assay. Bacteria (2x 10^4 CFU/100 µl DMEM) were incubated with 100µL of undiluted, immobilized, pooled mNL in presence of 0.1% BSA for 2hr at 30°C. After 19 washes, adherent bacteria were determined by resuspending with 0.001% Triton X-100 following plating on TS agar plates supplemented with 200 µg/ml streptomycin. **(A)** Prior to immobilization, mNL was sonicated (Amplitude 8µM) for increasing amounts of time followed by blocking with 0.1% BSA and incubation with Spn **(B)** Filtering of mNL's with a 0.45uM filter followed by immobilization, blocking with 0.1% BSA and incubation with Spn **(C)** Treatment of immobilized mNL with 100mM $NaIO_4$ in 50mM sodium acetate buffer for 30 min at 4°C in the dark followed by blocking with 0.1% BSA and incubation with Spn **(D)** Treatment of immobilized mNL with 50µg/mL trypsin for 30 min at 37°C followed by the blocking with 0.1% BSA and incubation with Spn. **(E-F)** Wild-type Spn were incubated with mNL or hNF for 2hr at 37°C and 5% CO_2. **(E)** Type 4 (TIGR4) incubated with mNL **(F)** Type 23F incubated with human nasal fluid (hNF). Mucus (blue) was stained with alcian blue and bacteria (green) were detected using rabbit anti-capsule antibody and secondary FITC-coupled goat anti-rabbit IgG. Spn were visualized by microscopy on an Axiovert 40 CFL microscope equipped with an Axiocam IC digital camera at 100x. Experiments were performed in duplicates and mean values of three independent experiments are shown with error bars corresponding to S.D. *,$p<0.05$; **,$p<0.01$ by Kruskal-Wallis test, followed by Dunn's multiple comparison test (A) or Mann-Whitney test (B,C, D).

Figure 2: Screening of pneumococcal surface factors interacting with mucus
Adherence of WT Spn and isogenic mutants to pooled mNL or hNF was assessed in a solid phase assay. Bacteria (2x 10^4 CFU/100µl DMEM) were incubated with 100µL of undiluted, immobilized, pooled mNL in presence of 0.1% BSA for 2hr at 30°C. After 19 washes, adherent bacteria were determined by resuspending with 0.001% Triton X-100 following plating on TS agar plates supplemented with 200 µg/ml streptomycin. **(A)** Adherence of TIGR4, TIGR4Δ*cps* and TIGR4Δ*cps::cps* to mNF. **(B)** Adherence of TIGR4 and TIGR4Δ*rlrA* to mNF. **(C)** Adherence of Type 23F and Type 23F::pilus-1 to hNF. Experiments were performed in duplicates and mean values of three independent experiments are shown with error bars corresponding to S.D. **,p<0.01; ****,p<0.0001 by 1-way ANOVA followed by Dunnett´s multiple comparison test for multiple comparison (A) or Mann-Whitney test (B,C).

Figure 3: NanB and NanA mediate mucus evasion
Adherence of WT Spn and isogenic mutants to pooled mNL and hNF was assessed in a solid phase assay. Bacteria (2 x 10^4 CFU/ 100 µl DMEM) were incubated with 100µL of undiluted, pooled mNL or 10 µg hNF in presence of 0.1 % BSA for 2hr at 30°C. After 19 washes, adherent bacteria were determined by resuspending with 0.001% Triton X-100 following plating on TS agar plates supplemented with 200 µg/ml streptomycin. **(A)** Adherence of Type 23F::pilus-1; Type 23F::pilus-1,*nanB::*janus and Type 23F::pilus-1,*nanB::nanB* to mNF **(B)** Adherence of Type 23F::pilus-1 and Type 23F::pilus-1,*nanB::*janus and Type 23F::pilus-1,Δ*nanA,nanB*::janus to hNF **(C)** Adherence of Type 23F::pilus-1 and Type 23F::pilus-1,-*nanB::*janus and Type 23F::pilus-1,$NanB_{D270A}$ to hNF **(D)** Adherence of Type 23F::pilus-1; Type 23F::pilus-1,Δ*nanA* and Type 23F::pilus-1,Δ*nanA::nanA* to mNF **(E)** Adherence of Type 23F::pilus-1; Type 23F::pilus-1,Δ*nanA* and Type 23F::pilus-1,Δ*nanA::nanA* to hNF**.** Experiments were performed in duplicates and mean values of three independent experiments are shown with error bars corresponding to S.D. *,p<0.05; ***,p<0.001; ****,p<0.0001 by 1-way ANOVA followed by Dunnett´s multiple comparison test or Mann-Whitney (B).

Figure 4: NanB regulates *nanA* in a sialic acid-dependent manner
(A-B) Neuraminidase activity by Spn was quantified using NA-STAR kit (Thermo-Fischer Scientific, USA). Pneumococcal isolates of different serotypes (**A**), or the defined isogenic mutants of Type 23F::pilus-1 (**B**)-were grown up to 1x10^8 CFU/mL, centrifuged and resuspended in PBS at a density of 10^7 CFU/mL. Bacterial suspensions were then sonicated (amplitude, 8 µm) and the supernatant incubated in buffer and NA-STAR substrate for 20 minutes at room temperature before reading the chemiluminescent signal. To analyze the data, the signal was divided by the noise (PBS control). Experiments were performed in duplicates and mean values of three independent experiments are shown with error bars corresponding to S.D.**,p<0.01; ****,p<0.0001 by ordinary 1-way ANOVA followed by Holm-Sidak's multiple comparison test. **(C-E)** Transcription level of *nan* genes was measured using quantitative RT-PCR. Spn strains were grown in TS at 37°C to OD_{620}=1.0 followed by RNA extraction. Data shown as the fold-change was calculated relative to parent strain (Type 23F::*pilus-1*) for **(C)** *nanB* **(D)** *nanA* **(E)** *nanR*. Mean values of two independent experiments performed

in duplicate are shown with error bars corresponding to S.D. **(F)** Neuraminidase levels and activity in response to sialic acid found in mNLs were also assessed using the NA-STAR kit. Type 23F::pilus-1 and isogenic mutants were grown in TS for 1hr, spun down and resuspended in DMEM. These samples were added at a 1:50 dilution to DMEM alone, or DMEM with mNL. They were incubated at 37°C and 5% CO_2 for 3 hours, centrifuged and resuspended in PBS. Samples were then treated in the same manner as Figure 4B. Experiments were performed in duplicate and mean values of 3 independent experiments are shown with error bars corresponding to S.D.****,p<0.0001 by 1-way ANOVA followed by Holm-Sidak's multiple comparison test.

Figure 5: NanB and NanA mediate mucus evasion through removal of sialic acid
(A) Adherence of WT Spn and isogenic mutants to pooled human nasal fluid (hNF) was assessed in a solid phase assay. Immobilized hNF (10µg) was pre-incubated with exogenous neuraminidase from lyophilized *Vibrio cholerae* or vehicle control (calcium saline) alone. **(B)** The ability of WT Spn and isogenic mutants to remove sialic acid from mucus was quantified by ELISA. hNF was immobilized in a microtiter plate incubated with bacteria (1 x 10^6 CFU/100 µl DMEM) for 4hr at 37°C. Binding of biotinylated lectin Mal-II to α-2,3 sialic acid was detected using peroxidase-coupled streptavidin. The values of control wells without hNF were subtracted from each measured value. Results are illustrated as % of control of hNF of two independent experiments with 4 wells each. **(A-B)** Experiments were performed in duplicates and mean values of three independent experiments are shown with error bars corresponding to S.D. *, p<0.05;**,p<0.01, ***;p<0.001; ****, p<0.0001 by a T-test comparing to respective vehicle controls (A) and by 1-way ANOVA followed by Dunnett´s multiple comparison test (B).

Figure 6: Effect of neuraminidases on colonization *in vivo*
(A) Adult mice were intranasally infected with a suspension containing equal amounts of wild-type and isogenic double neuraminidase mutant. Colonization density) was assessed 4 hr and 24 hr p.i. in the URT lavages to calculate the competitive index (CI**).** Dotted line represents CI = 1. Group medians were compared to a CI = 1 by Wilcoxon signed rank test and resulting p-values are indicated.**(B)** Infant and adult mice were intranasally infected with wild-type and an isogenic double neuraminidase mutant. Colonization density was assessed at 4hr and 24hr p.i. in adult mice and 5 days p.i. in infant mice. Experiments were repeated twice and groups represent n=5 –15 animals with error bars corresponding to S.D. ****, p<0.0001 by Mann-Whitney test.

Figure 7: Spn neuraminidases stimulate mucus containing secretions in a neuraminidases-dependent manner
(A) URT tissue sections of mock- or Spn-infected infant mice were examined at day 5 post-infection. Sialic acid containing secretions were visualized through a SNL lectin staining that detects α-2,6 linked sialic acid (upper row) or alcian blue-PAS staining for mucopolysaccharides (lower row). **(B-C)** To quantify sialic acid and mucus containing secretions in the URT of mice, retro-tracheal lavages were obtained from infant mice at day 5 post-infection. Immunoblots were performed with the lavages to determine the amount of α-2,6 linked sialic acid **(B)** or the MUC5A/c mucin **(C)**. Experiments were performed in duplicates and mean values of three independent experiments are shown

1002 with error bars corresponding to S.D., **,p<0.01, ***,p<0.001 by 1-way ANOVA followed
1003 by Dunnett´s multiple comparison test or Mann-Whitney.
1004

Figure 1

Figure 2

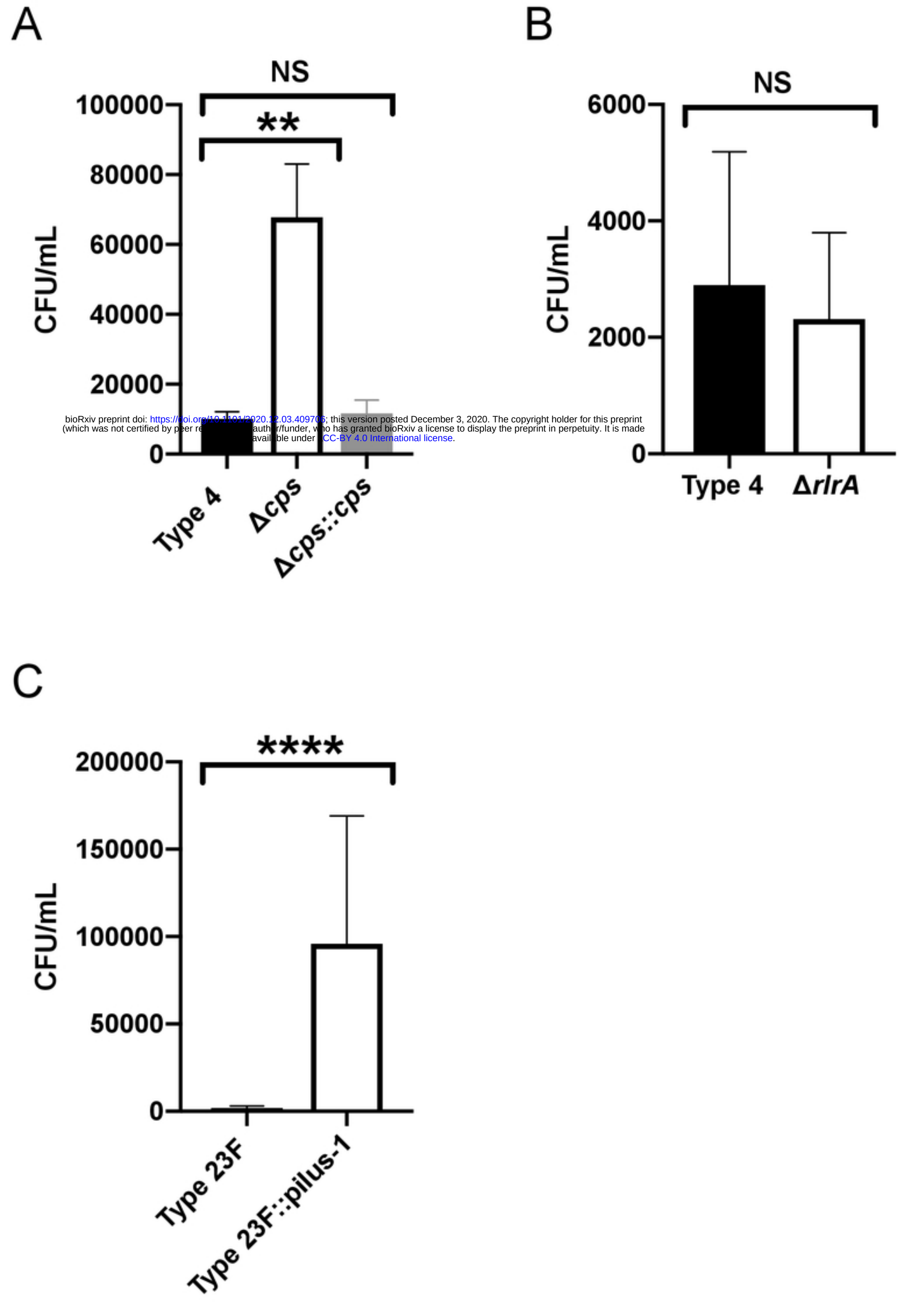

Figure 3

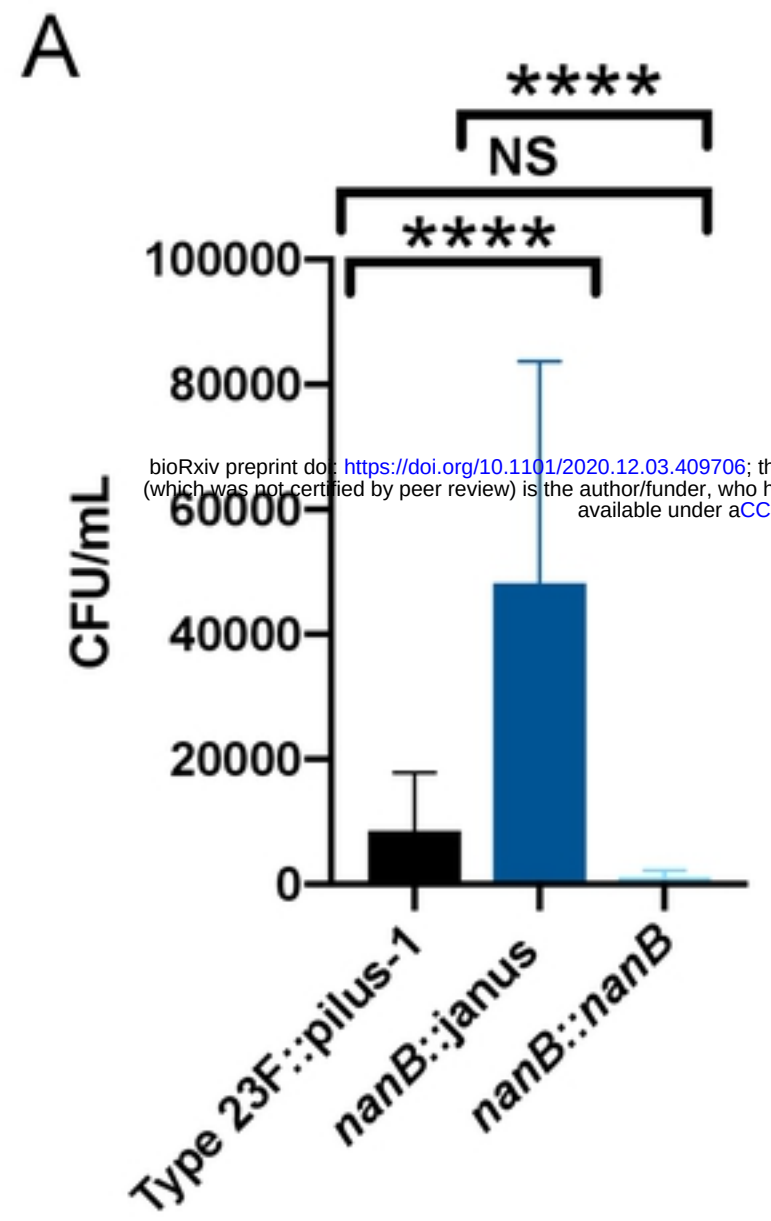

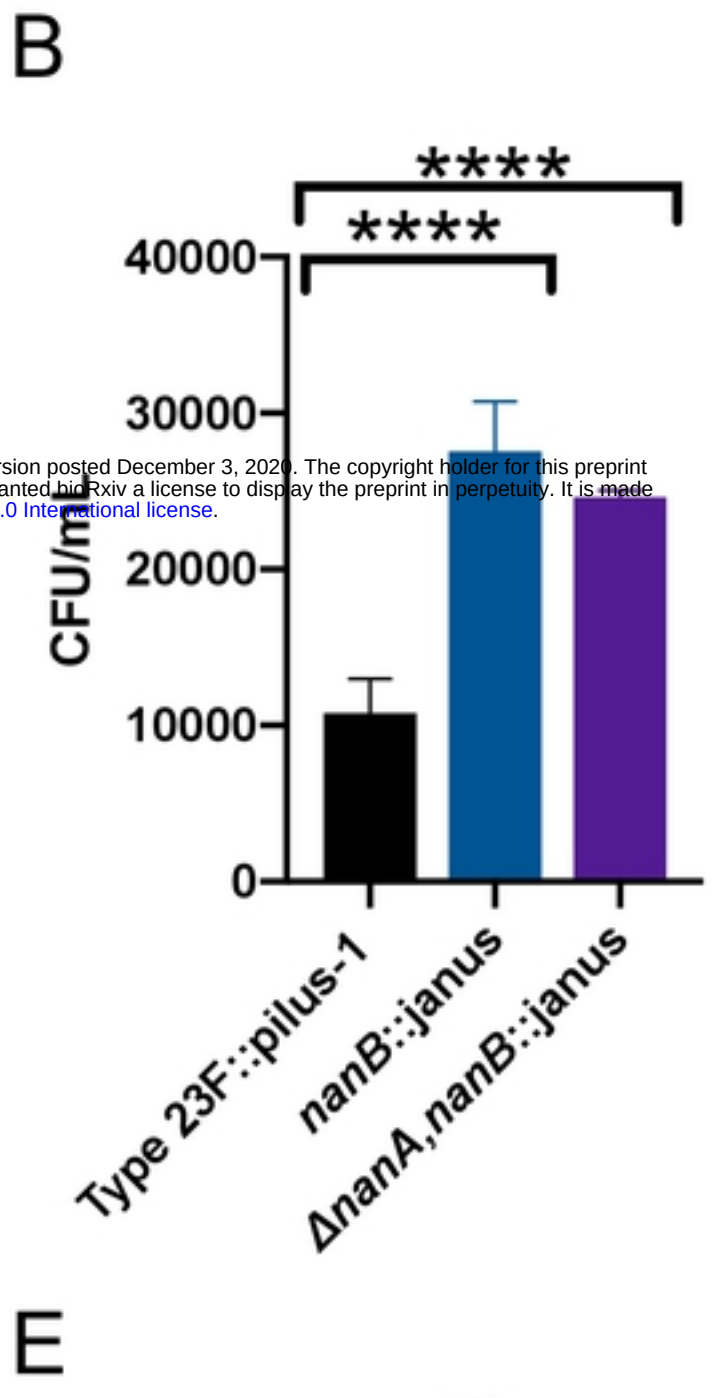

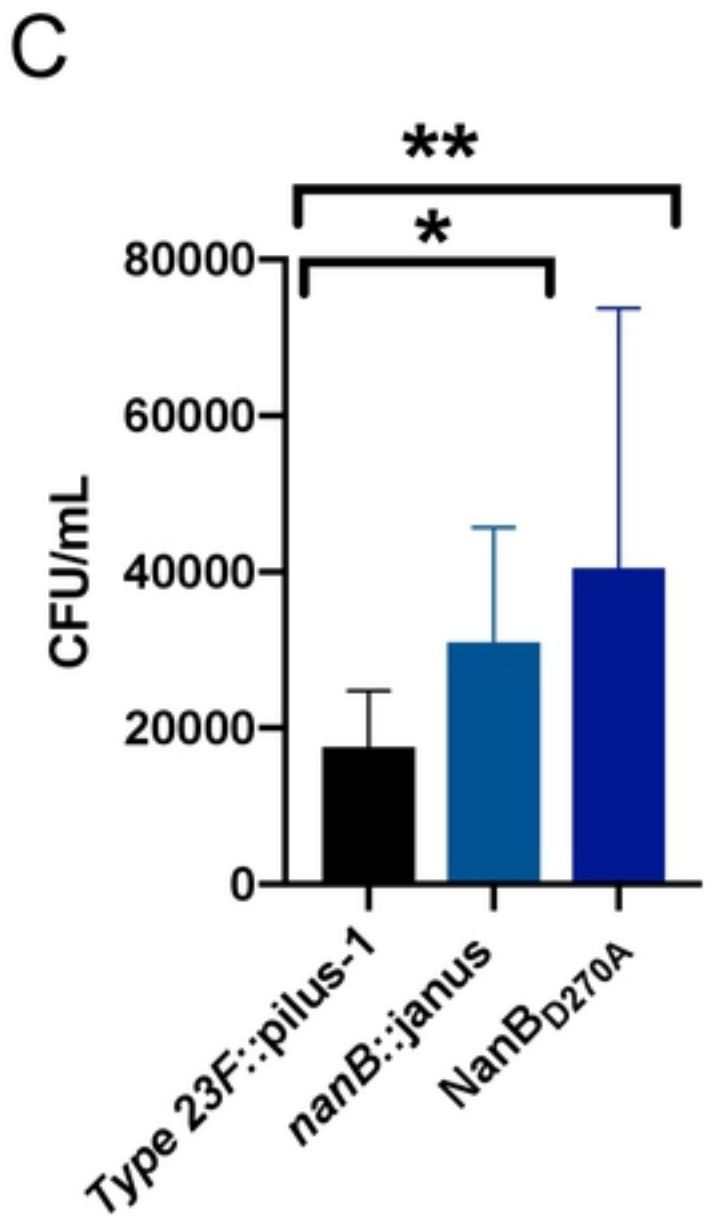

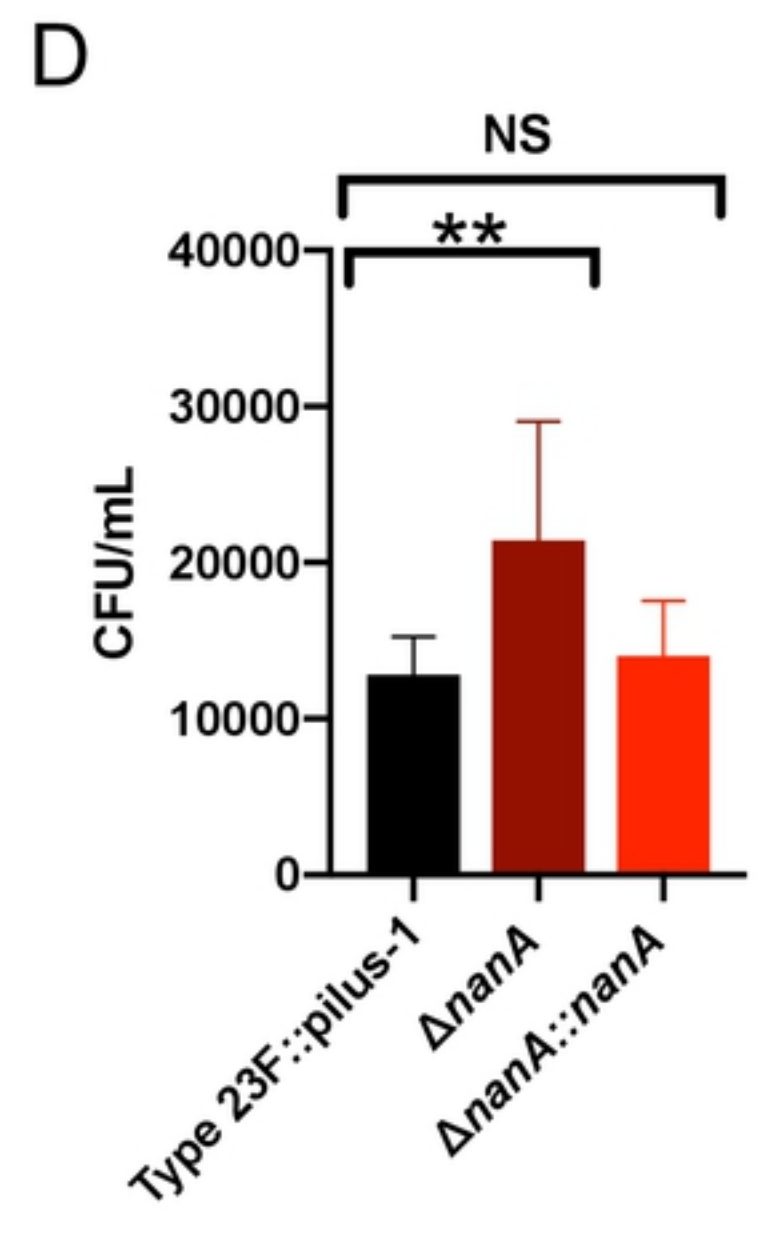

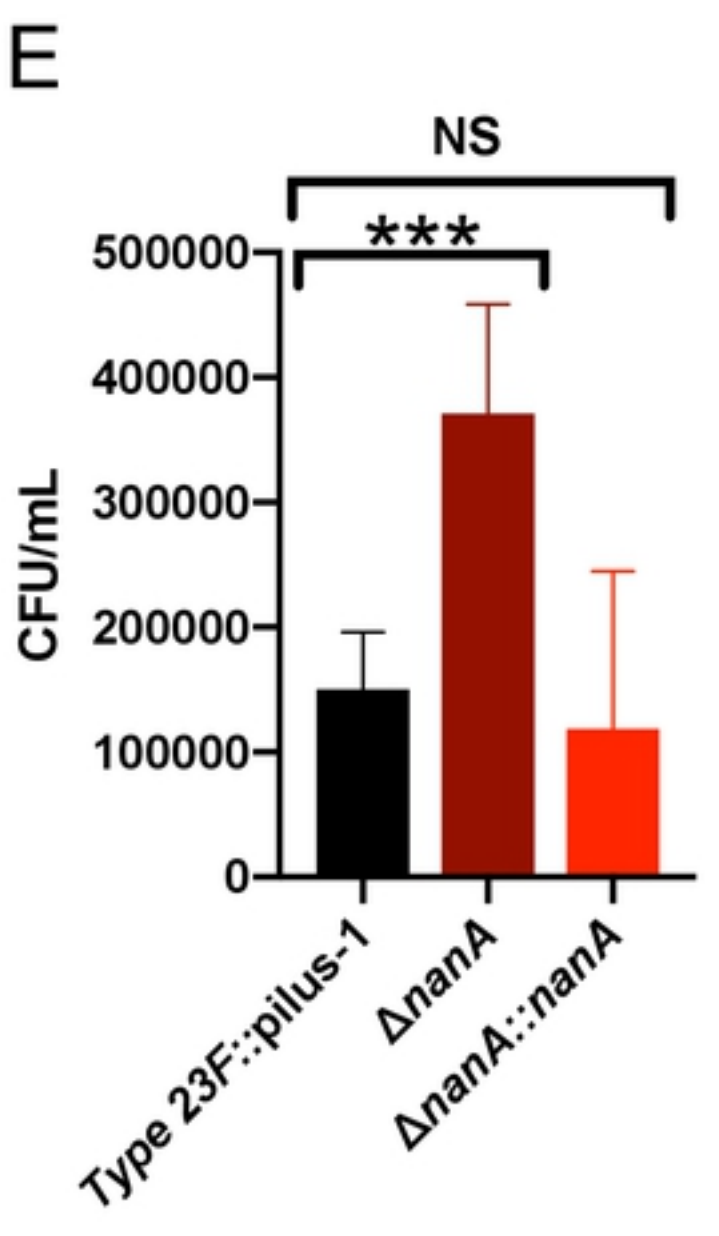

Figure 4

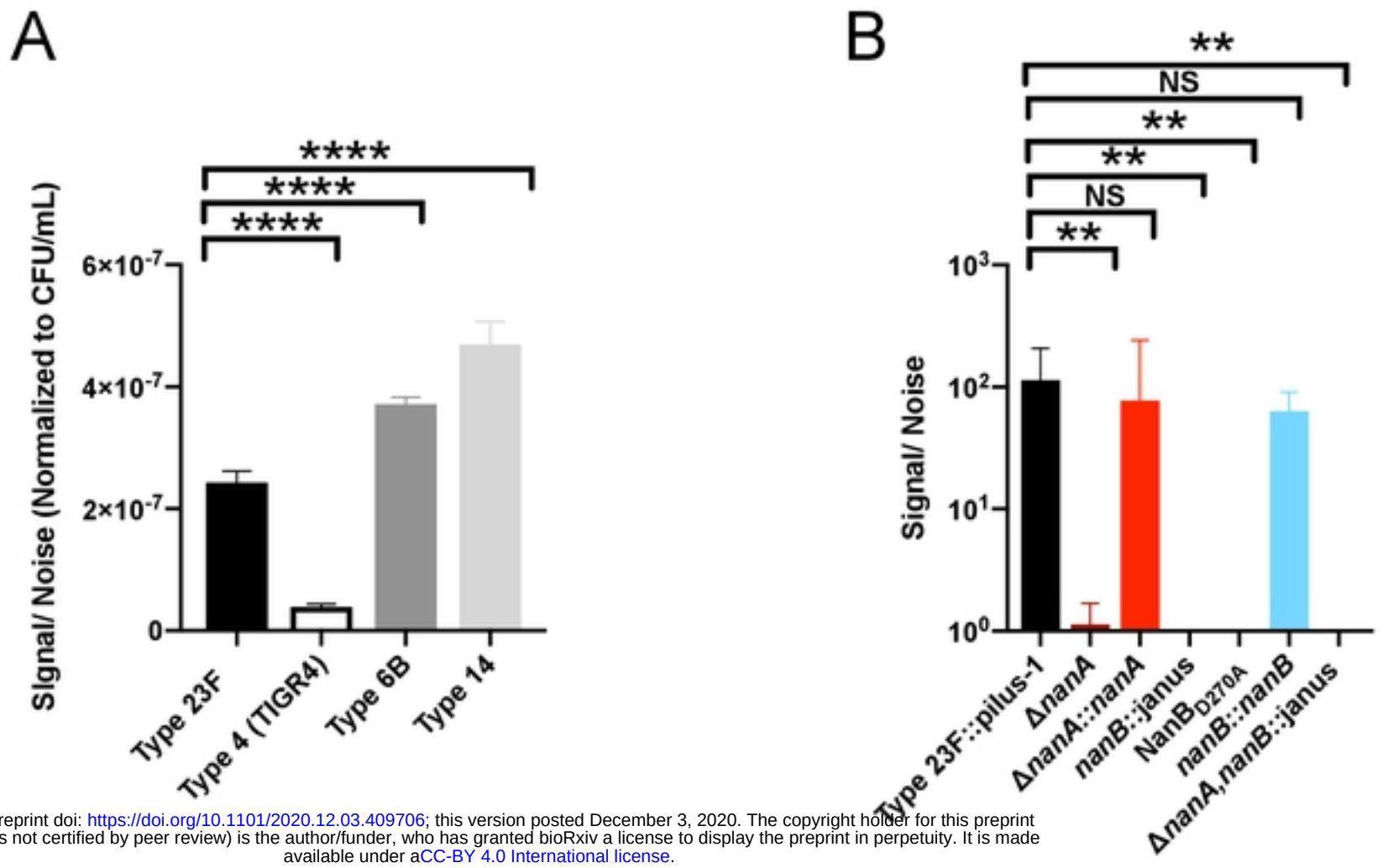

Figure 5

A

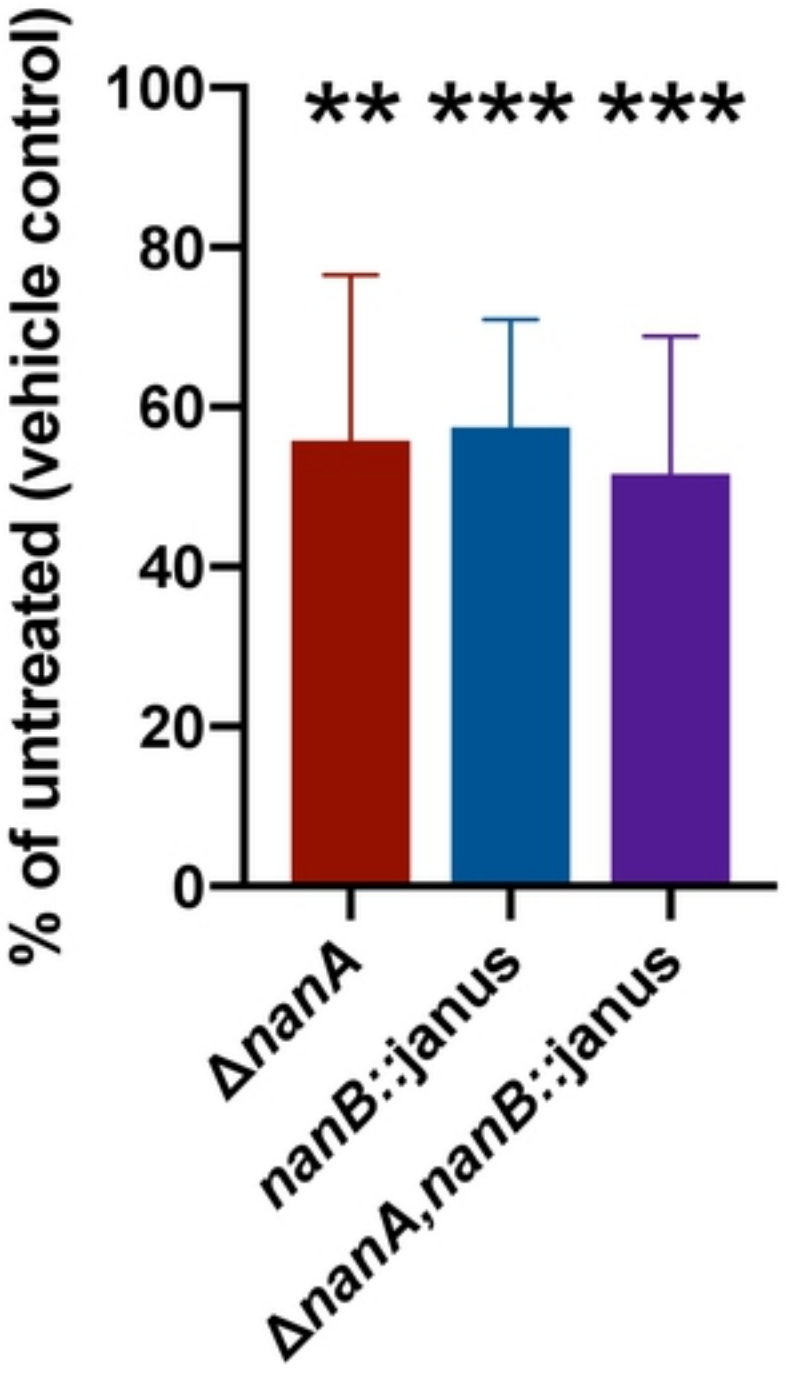

B

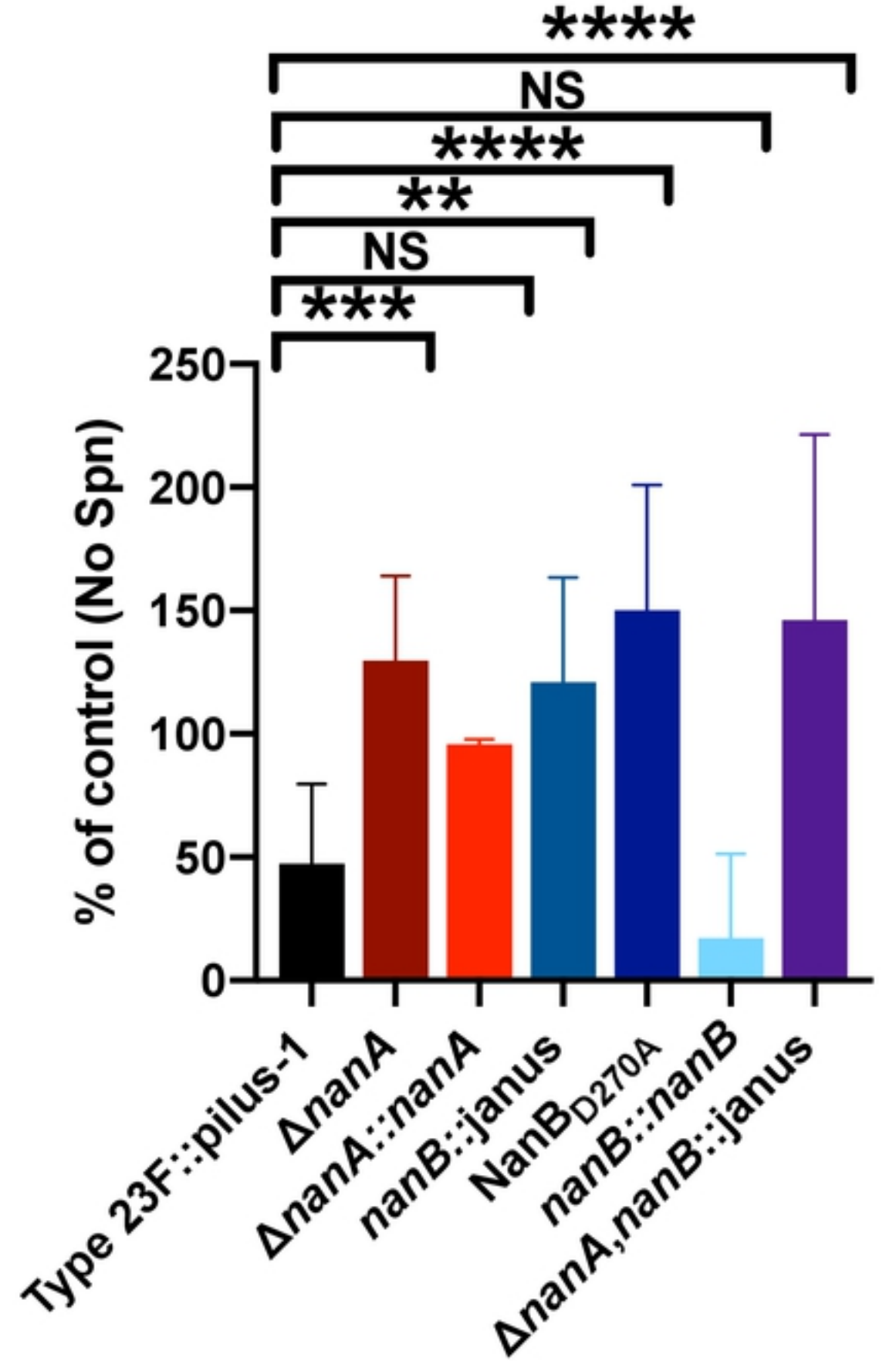

Figure 6

A

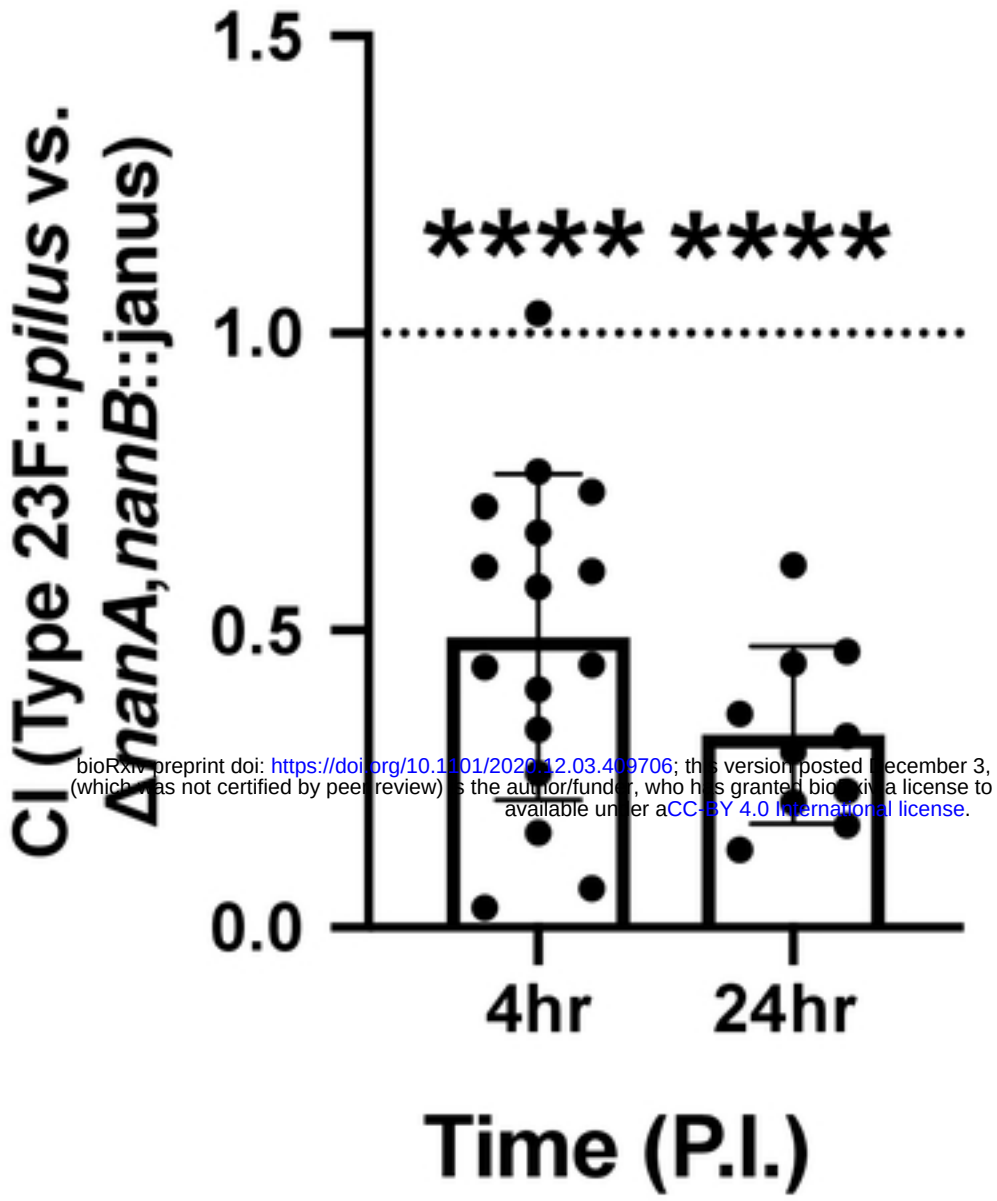

B

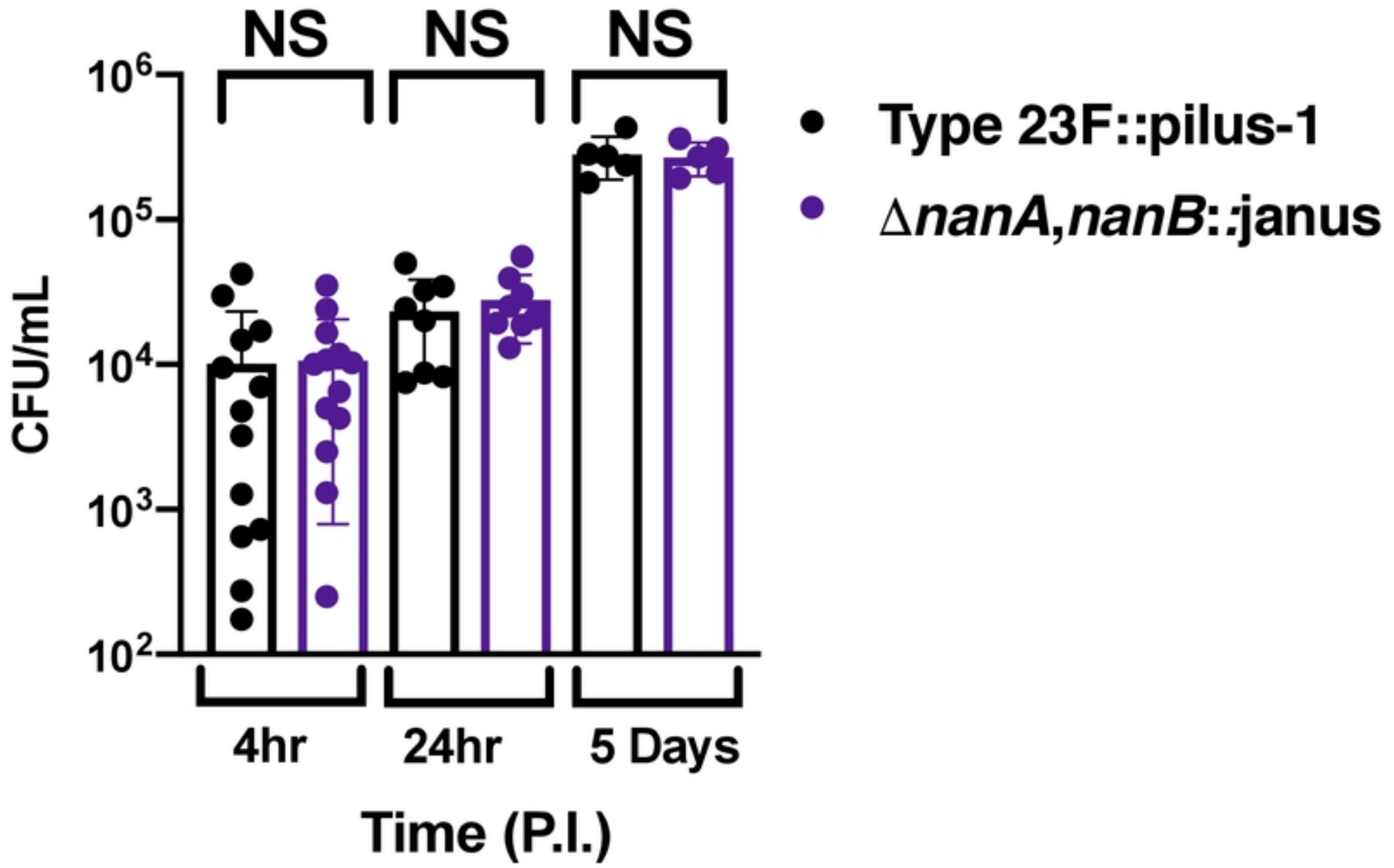

Figure 7

A

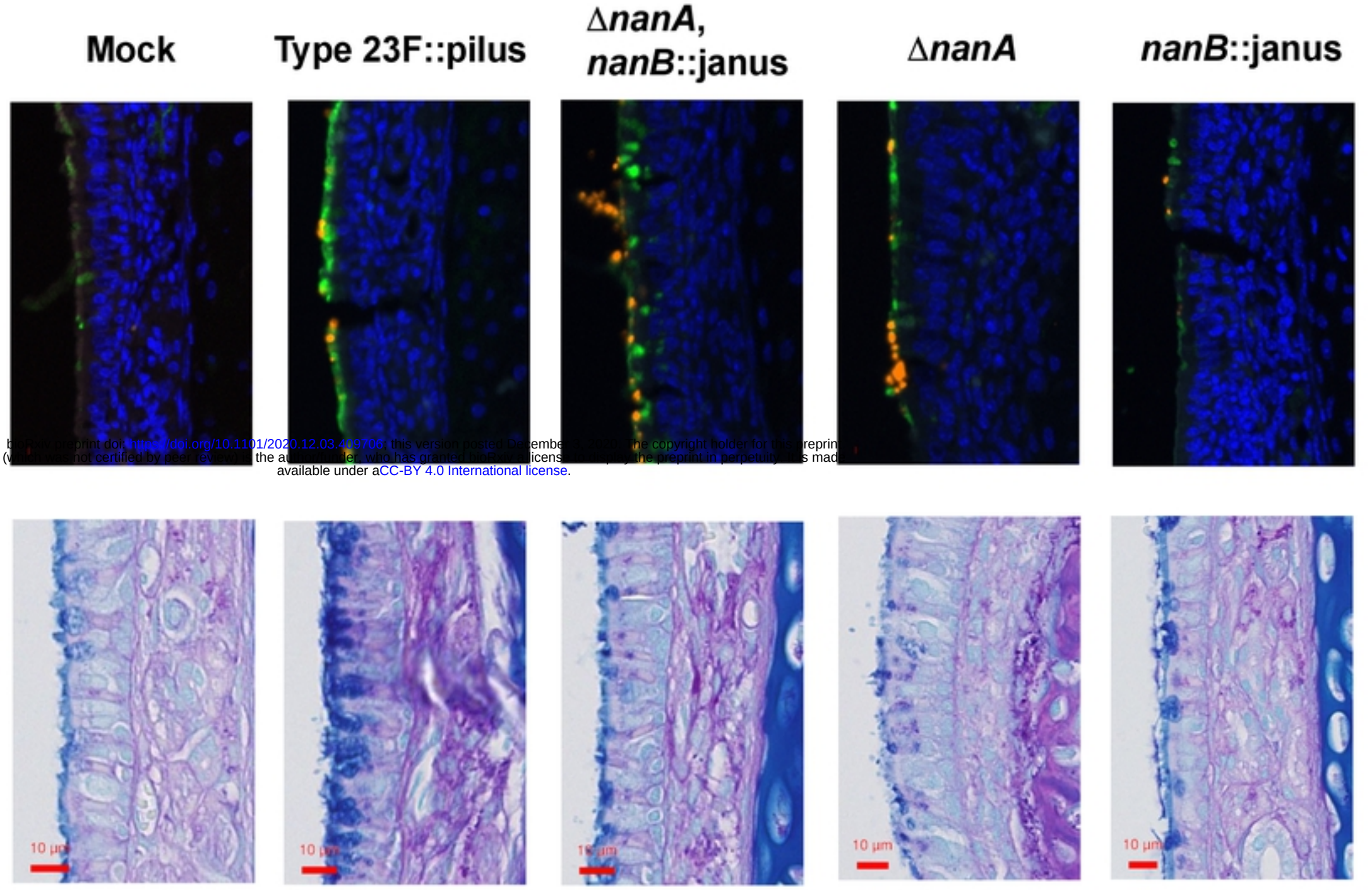

B

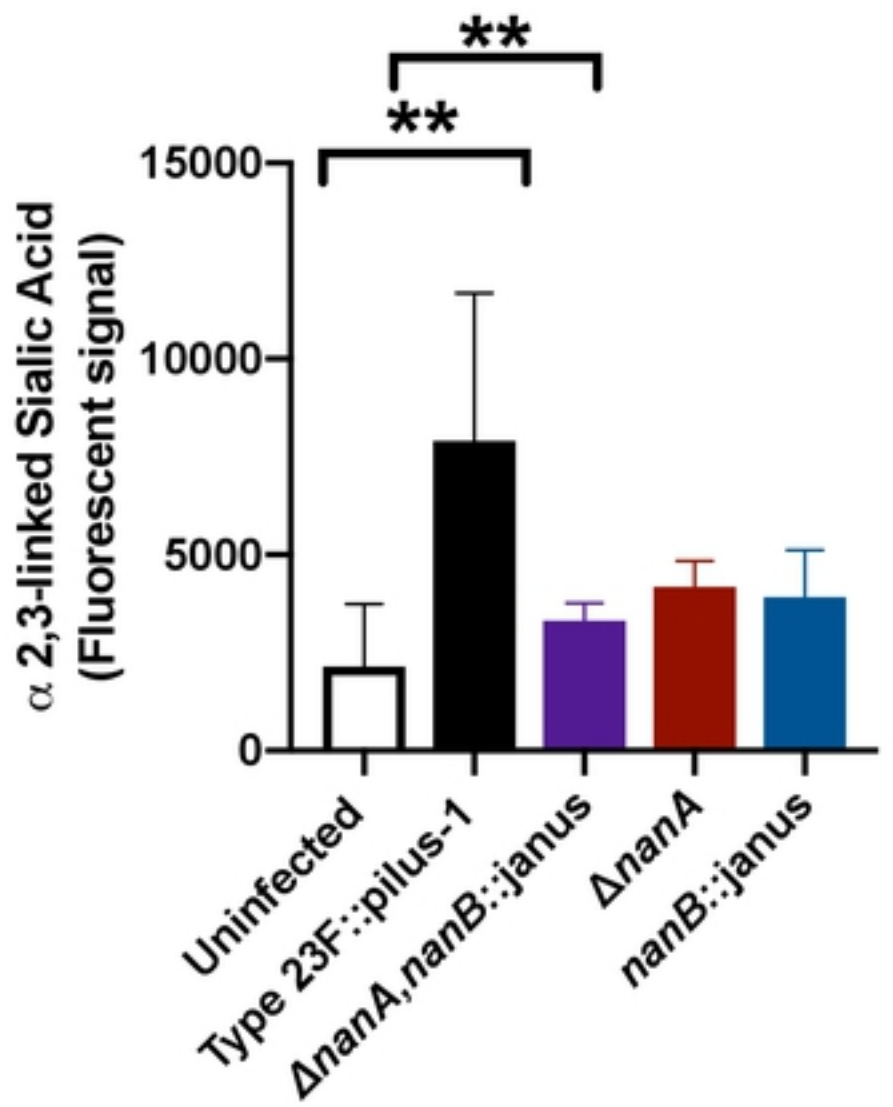

C